Eur. Phys. J. C (2024) 84:1028
https://doi.org/10.1140/epjc/s10052-024-13434-w

THE EUROPEAN PHYSICAL JOURNAL C

Check for updates

Regular Article - Theoretical Physics

ϕ meson mass and decay width in magnetized strange hadronic matter

Nisha Chahal[1,a], **Rajesh Kumar**[2,b], **Suneel Dutt**[1,c], **Arvind Kumar**[1,d]

[1] Department of Physics, Dr. B. R. Ambedkar National Institute of Technology Jalandhar, Punjab 144008, India
[2] Department of Physics, Centre for Nuclear Research, Kent State University, Kent, OH 44243, USA

Received: 24 June 2024 / Accepted: 30 September 2024
© The Author(s) 2024

Abstract We investigate the medium modifications in mass and decay width of ϕ meson in the presence of an external magnetic field. The in-medium mass of ϕ meson has been calculated using the decay process $\phi \to K\bar{K}$ at one-loop level. The medium modifications are introduced by using a chiral SU(3) model employing a mean-field effective approach. Due to the introduction of the magnetic field, masses of charged K^+ and K^- increases with advancing magnetic field values. A negligible change in the value of neutral K^0 and $\bar{K}^0$ has been observed for varying magnetic fields. Due to electromagnetic interactions with charged K and $\bar{K}$ mesons, there is a gradual augmentation in the effective mass of ϕ meson. The probability of the mentioned decay process ceases to be zero for low density and strangeness fraction values at higher magnetic field values. Investigating the decay width and effective mass of ϕ meson under the influence of an external magnetic field is relevant to understanding the hadronic matter properties under extreme conditions achievable at heavy-ion collision experiments.

1 Introduction

Investigating the thermodynamic properties of hadrons in the asymmetric strange matter at finite density and temperature values is of significant importance in strong interaction physics, particularly in exploring the quark-gluon plasma (QGP) [1–11]. Experimental facilities such as the Relativistic Heavy Ion Collider (RHIC) [12,13] at Brookhaven National Laboratory (BNL) and the Large Hadron Collider (LHC) at CERN [14,15], the European Organization for Nuclear Research, are pioneers in exploring the different regimes of quantum chromodynamics (QCD) phase diagram. Future experiments such as the Facility for Antiproton and Ion Research (FAIR) [16,17] and the Nuclotron-based Ion Collider facility (NICA) [18] are poised to make notable advancements by systematically exploring the hot and dense matter. When asymmetric atomic nuclei collide at high energies, they cause the formation of QGP, which is followed by a rapid expansion of the resulting fireball due to the extremely high pressures and temperatures involved [19–21]. As the fireball of QGP expands and cools, it undergoes a phase transition known as hadronization, where quarks and gluons recombine to form nucleons (protons and neutrons), hyperons (particles containing strange quarks), and mesons (particles consisting of quark-antiquark pairs) [22–24]. Studying the properties of hadronic matter produced in heavy ion collisions (HICs) helps to deepen the understanding of fundamental aspects of QCD, such as confinement and chiral symmetry breaking. It sheds light on the evolution of the early universe, where similar conditions are believed to have prevailed shortly after the Big Bang [25,26].

Various theoretical frameworks have been constructed to comprehend the characteristics of hadrons within the non-perturbative domain. The primary findings from lattice QCD simulations have suggested a smooth crossover transition from the confined hadronic phase to the deconfined quark-gluon plasma at low or zero chemical potential with increasing temperature value [27–29]. For higher chemical potential values, the partition function involves complex phase factors due to the fermionic nature of quarks, leading to oscillatory terms that can cancel each other when performing numerical simulations, resulting in increased computational costs and lower efficiency [30,31]. As a result, lattice QCD at high chemical potentials becomes computationally demanding and less reliable, limiting its applicability in studying QCD matter at extreme conditions. Addressing the fermion

[a] e-mail: nishachahal137@gmail.com
[b] e-mail: rkumar6@kent.edu
[c] e-mail: dutts@nitj.ac.in
[d] e-mail: kumara@nitj.ac.in (corresponding author)

Published online: 08 October 2024

sign problem in lattice QCD simulations at finite chemical potential involves strategies such as performing simulations at imaginary chemical potentials and analytically continuing the results, using Taylor expansion techniques, employing reweighting methods, and exploring alternative formulations like dual representations of QCD [32,33]. To explore the QCD phase diagram beyond the lattice QCD regime, several phenomenological models and approaches like hadron resonance gas (HRG) model [34], Nambu–Jona–Lasinio (NJL) model [35], linear-sigma model (LSM) [36], quark-meson (QM) model [37], quark meson coupling (QMC) model [38], Dyson–Schwinger equation approach [39] and the coupled-channel approach [40] based on fundamental QCD principles have been developed to investigate the characteristics of hadrons. To study the deconfinement transition along with the chiral symmetry restoration, NJL is extended to PNJL [41], LSM to PLSM [42], and QM model to PQM [43] by the inclusion of Polyakov loop potential [44]. Theoretical studies have expanded their focus to consider various factors, such as the influence of external magnetic fields [45–47], the implications of finite system sizes [48–50], the exploration of non-extensive properties, including long-distance correlations [51,52], and investigating the effects of electrical fields on the thermodynamics of strongly interacting matter [53,54].

The relation between medium modifications of masses and chiral symmetry restoration is complex and has been a significant topic of study for around two decades, theoretically and experimentally. These approaches attempt to describe the behavior of baryons and mesons in dense and hot environments and their implications for observable quantities, such as the equation of state. Due to the challenges in definitively understanding the behavior of the ρ meson at finite density and its relationship to chiral symmetry [55,56], the focus has shifted towards mesons with narrower widths, such as ϕ meson [35,57–65]. This is attributed to the fact that vector mesons are particularly advantageous for experimental investigations of in-medium effects because they can decay into dileptons [66–72], which are insensitive to the strong interactions and hence less influenced by the surrounding nuclear medium than hadronic decay products. The quark content of K mesons, involving combinations of u, d, and s quarks, provides insights into the mechanisms of mass generation and investigating CP violation, which partly addresses the universe's matter–antimatter asymmetry. The presence of strange quarks in the QGP results in enhanced production of strange hadrons, including kaons, providing a unique window into the medium's characteristics. By analyzing the ratio of strange to non-strange hadrons, such as the K/π ratio, researchers can discern deviations from expected patterns, signaling the presence of QGP and the onset of deconfinement [73,74]. The strong interaction between ϕ ($s\bar{s}$) mesons and u, d quarks arises from loop contribution of $K\bar{K}$ pairs, highlighting the importance of the in-medium characteristics of kaons and antikaons [75–80]. The ϕ meson primarily facilitates the annihilation process of $K\bar{K}$ into a dilepton, which provides valuable insights into understanding the behavior of the ϕ meson within dense hadronic medium [81–84]. Investigating the mass and width of the ϕ meson in nuclear matter using an effective Lagrangian approach within the QMC model, a downward mass shift of ϕ meson was observed with broadened decay width [35,85,86]. In the framework of chiral perturbation theory, incorporating the medium-induced change in kaon mass and including loop corrections has been shown to significantly impact the properties of ϕ meson within dense matter, particularly evident when the kaon mass diminishes [67]. The production of ϕ mesons has been examined experimentally by studying the invariant mass spectra of dimuon through the collision of protons/sulfur projectiles at 200 GeV/nucleon with tungsten/uranium targets by HELIOS-3 Collaboration and the NA38 Collaboration at CERN/SPS [87,88]. Findings from the KEK-E325 collaboration indicated a notable decrease in the mass of the ϕ meson, amounting to approximately 3.4%. Additionally, they observed an in-medium decay width of around 14.5 MeV under conditions of saturation nuclear matter density by analyzing the invariant mass spectra of e^+e^- pairs generated by $p+A$ collisions [59]. Thus, the interplay between theory and experiment elucidates intricate details of ϕ meson's properties, such as production, propagation, and decay width, deepening our comprehension of QGP, CP-violation, and chiral symmetry breaking.

A finite magnetic field has been anticipated to be present in the early universe conditions [89], magnetars [90], and during HICs in particle accelerators at LHC and RHIC [91,92]. Understanding the phase diagram of QCD under finite magnetic field strengths and non-zero chemical potentials is crucial in these contexts. The magnitude of magnetic fields varies widely across different scenarios, ranging from estimates as high as eB around $200m_\pi^2$ in the early universe [89,93,94] to values around $15m_\pi^2$ at the LHC [95,96]. Also, it has been demonstrated that holography sets a limit on the maximum intensity of magnetic fields, reaching approximately 3.6×10^{18} gauss at the temperature of hadronization [97]. The QCD phase diagram has been studied in the NJL/PNJL model by considering the magnetic field-dependent coupling constant [98]. External magnetic fields significantly influence the interaction of valence and sea quarks in quark matter [99–101]. A system possessing a nonzero chirality responds to a magnetic field by inducing a current aligned with the field, named the "chiral magnetic effect" (CME). Experimental investigation of the CME can be conducted through HICs, where its observation would directly confirm the presence and importance of gluon configurations with non-trivial topology [13,102]. For very high magnetic fields and the lowest Landau level approximation,

it has been noted that the presence of a strong magnetic field leads to a modification of the shear viscosity to entropy ratio for neutral hadrons, owing to their interactions with charged particles [103,104]. In the study of mixing effects in vector and neutral pseudoscalar mesons in the two-flavored NJL model in the Landau gauge, a considerable reduction in mass of the lightest states has been reported [105]. Furthermore, introducing external parallel electric and magnetic fields in the NJL quark model has influenced the critical temperature of chiral symmetry restoration [54]. Additionally, the investigation of in-medium normalized masses of axial vector, pseudoscalar, and scalar meson states in magnetized quark matter through the determination of quark condensates and deconfinement order parameters in a mean-field approximation provides further insights into the complex dynamics of meson systems [106]. Using the mean-field approximation method, the study in Ref. [107] observed a significant rise in the effective mass of K^0 mesons as baryonic density increased. Meanwhile, the decay width of ϕ meson changes dramatically with magnetic field strength, particularly leading to the obstruction of the K^+K^- decay channel beyond a certain critical magnetic field strength.

Lattice QCD simulations have reported a decrease in critical temperature as the magnetic field strength increases, termed as "inverse magnetic catalysis" [101]. This effect has also been observed in phenomenological investigations that account for contributions from a magnetized Dirac sea [108]. The investigation of the Walecka model incorporating a magnetized Dirac sea of nucleons with finite anomalous magnetic moments has shown inverse magnetic catalysis [109]. Additionally, the chiral SU(3) model has been utilized to examine properties of D mesons, charmonium, and spectral properties of vector mesons, incorporating contributions from a magnetized Dirac sea [110,111]. Our current manuscript does not incorporate these contributions for ϕ meson properties. Investigating the in-medium properties of mesons in a finite external magnetic field holds significant importance in analyzing the behavior of hadronic matter in different physical scenarios.

In the current work, we present findings concerning the mass and decay width of the ϕ meson within asymmetric strange hadronic matter in the presence of an external magnetic field. This is achieved by considering the influence of medium-induced masses for kaons using the chiral SU(3) model framework. The masses of K and $\bar{K}$ mesons are calculated at varying densities and temperatures in the strange hadronic matter to determine further the medium-modified mass and decay width of ϕ meson. The chiral SU(3) model has been extensively used to study various aspects of hadron physics, including the properties of mesons and baryons in vacuum and medium, as well as their interactions in different environments such as nuclear matter or hot and dense quark-gluon plasma [112–115]. In the study of charged $K^{\pm}$ mesons in magnetized nuclear matter, it has been observed that there are additional positive shifts in their mass when subjected to a magnetic field originating from the lowest Landau level [116]. Studying the dynamics of kaons and antikaons in more realistic conditions like HICs, including hyperons, introduces an additional degree of freedom associated with strangeness, helping constrain the EOS. Also, the extension to a finite magnetic field, which has been predicted in extreme temperature and density conditions, gives a more precise prediction of the behavior of ϕ meson in such environments.

The structure of this paper is organized as follows: In Sect. 2.1, we have provided a brief overview of the methodology employed to derive the in-medium scalar and vector fields within magnetized hadronic matter. The introduction of the magnetic field in the model and its impact on charged and uncharged baryons have been described in Sect. 2.2. Section 2.3 is dedicated to compute the in-medium masses of kaons and antikaons through the interactions facilitated by the chiral model fields, thus calculating the effective mass and decay width of the ϕ meson. Section 3 presents a detailed discussion of the quantitative results derived from our investigations. Finally, we have encapsulated our findings and contributions in Sect. 4, offering a comprehensive conclusion to our study.

2 Methodology

In the present work, the chiral SU(3) model is used to investigate the impact of the external magnetic field on the masses of kaons and antikaons. The isospin asymmetry and strangeness fraction influence both scalar and vector fields. Additionally, we employ a self-consistent Lagrangian approach to compute the mass and decay width of the ϕ meson. In the upcoming sections, we will provide a concise overview of the formalism employed to derive the scalar and vector fields in the presence of a magnetic field.

2.1 The hadronic chiral SU(3) model

The hadronic chiral model is based on broken scale invariance and non-linear realization of chiral symmetry and is employed to investigate hadron-hadron interactions [117, 118]. This model considers a mean-field approximation, a non-perturbative relativistic method that offers an approximate solution to the nuclear many-body problem. Within this approximation, all meson fields are treated as classical fields, with only vector (V) and scalar (S) fields contributing to the Lagrangian term of the baryon-meson interactions due to the zero expectation value of other mesons [117]. In particular, ρ and δ fields account for isospin asymmetry within the hadronic medium, whereas the strange scalar meson field, ζ, and strange vector field, ϕ, are introduced in the model

to account for the strangeness in the medium. Furthermore, introducing the dilaton field χ allows us to express the scale symmetry-breaking property of QCD, resulting in a non-vanishing trace of the energy-momentum tensor [115,119]. This comprehensive framework provides a foundation for exploring chiral hadronic matter under various conditions, providing insight into the scale symmetry, chiral dynamics, and isospin asymmetry at finite density and temperature [120,121]. The total mean-field Lagrangian density of the model is represented as

$$\mathcal{L}_{\text{chiral}} = \mathcal{L}_{\text{kin}} + \sum_{M=S,V} \mathcal{L}_{\mathcal{B}M} + \mathcal{L}_{\text{vec}} + \mathcal{L}_0 + \mathcal{L}_{\text{esb}}. \tag{1}$$

The first term in the above equation denotes the kinetic energy term that can be expressed as [122–124]

$$\begin{aligned}\mathcal{L}_{\text{kin}} = i\,\text{Tr}\,\bar{\mathcal{B}}\gamma^\mu D^\mu \mathcal{B} + \frac{1}{2}\text{Tr}\,D_\mu S D^\mu S + \text{Tr}\,(u_\mu S u^\mu S + S u^\mu u_\mu S) \\ + \frac{1}{2}\text{Tr}\,D_\mu Y D^\mu Y + \frac{1}{2}D_\mu \chi D^\mu \chi - \frac{1}{4}\text{Tr}\,(V_{\mu\nu}V^{\mu\nu}) \\ - \frac{1}{4}\text{Tr}\,(A_{\mu\nu}A^{\mu\nu}).\end{aligned} \tag{2}$$

Here, $\mathcal{B}$ represents the multiplet of baryon fields, S stands for the scalar meson multiplet, Y denotes the pseudoscalar singlet, χ is the scalar-isocalar dilaton field, $V_{\mu\nu} = D_\mu V_\nu - D_\nu V_\mu$ is the vector meson field tensor and $A_{\mu\nu} = D_\mu A_\nu - D_\nu A_\mu$ is the axialvector field tensor. In the above equation, the covariant derivative of fields $\mathcal{F} = \mathcal{B}, S, Y, A_\mu, V_\mu$ is defined as $D_\mu \mathcal{F} = \partial_\mu \mathcal{F} + i\left[\Gamma_\mu, \mathcal{F}\right]$, where $\Gamma_\mu = -\frac{i}{4}\left[u^\dagger \partial_\mu u - \partial_\mu u^\dagger u + u\partial_\mu u^\dagger - \partial_\mu u u^\dagger\right]$. Here u is the unitary transformation operator, represented as $u = \exp\left[\frac{i}{2\sigma_0}\pi^a \lambda^a \gamma_5\right]$ and $u_\mu = -\frac{i}{2}\left[u^\dagger \partial_\mu u - u\partial_\mu u^\dagger\right]$. The second term in Eq. (2) represents the kinetic energy term for the scalar mesons whereas the third term is for the pseudoscalar mesons. The pseudoscalar singlet field, Y, does not depend on the octet and thus has its kinetic term (fourth term in Eq. (2)). Last three terms are the kinetic terms for dilaton field χ, the vector and axial vector mesons, respectively [122].

The second term of Eq. (1) accounts for the interactions of baryons with scalar and vector mesons. Considering the general meson field ($M = S, V$), this term is defined as [122,123]

$$\begin{aligned}\mathcal{L}_{\mathcal{B}M} = -\sqrt{2}g_8^M \left(\alpha_M [\bar{\mathcal{B}}\mathcal{O}\mathcal{B}M]_F \right. \\ \left. + (1-\alpha_M)\,[\bar{\mathcal{B}}\mathcal{O}\mathcal{B}M]_D\right) - g_1^M \frac{1}{\sqrt{3}}\mathbf{Tr}(\bar{\mathcal{B}}\mathcal{O}\mathcal{B})\text{Tr}M.\end{aligned} \tag{3}$$

Due to the interaction with scalar fields, the effective mass of baryons gets modified as $m_i^* = -g_{\sigma i}\sigma - g_{\zeta i}\zeta - \tau_{3i}g_{\delta i}\delta$, where i denotes the baryons, p, n, Λ, Σ^0, Σ^+, Σ^-, Ξ^0, and Ξ^-. Similarly, as a consequence of the interplay between vector mesons (ω, ρ, ϕ) and baryons, the effective chemical potential of a single particle is defined by $\mu_i^* = \mu_i - g_{\omega i}\omega - \tau_{3i}g_{\rho i}\rho - g_{\phi i}\phi$. The symbol τ_{3i} represents the quantum number corresponding to the third component of isospin for a given particle, and $g_{\sigma i}$, $g_{\zeta i}$, $g_{\delta i}$, $g_{\omega i}$, $g_{\rho i}$ and $g_{\phi i}$ gives the coupling strength of baryons with scalar and vector mesons, respectively.

The term $\mathcal{L}_{\text{vec}}$ in Eq. (1) represents the interactions of vector mesons. In scale-invariant form, which implies the mass degeneracy of meson nonet, it is written as

$$\mathcal{L} = \frac{1}{2}m_V^2 \frac{\chi^2}{\chi_0^2}\text{Tr}(V_\mu V^\mu) + 2g_4\text{Tr}(V_\mu V^\mu)^2. \tag{4}$$

The first term in the above equation is made scale invariant by multiplying it with appropriate powers of dilaton field, χ. Explicitly, in terms of vector mesons ω, ρ and ϕ, the above equation is written as

$$\begin{aligned}\mathcal{L}_{\text{vec}} = \frac{1}{2}\left(m_\omega^2\omega^2 + m_\rho^2\rho^2 + m_\phi^2\phi^2\right)\frac{\chi^2}{\chi_0^2} \\ + g_4\left(\omega^4 + 6\omega^2\rho^2 + \rho^4 + 2\phi^4\right).\end{aligned} \tag{5}$$

The self interactions of the scalar mesons is governed by $SU(3)_V$ symmetry in the non linear realization of the chiral symmetry [123]. However, there are only three existing independent invariants given as $I_1 = \text{Tr}(S)$, $I_2 = \text{Tr}(S^2)$, $I_3 = \det(S)$. These invariants act as building blocks for all meson-meson interaction terms. The term $\mathcal{L}_0$ in Eq. (1) regulates the phenomena associated with spontaneous chiral symmetry breaking and is written in terms of I_1, I_2 and I_3 as

$$\mathcal{L}_0 = -\frac{1}{2}k_0\chi^2 I_2 + k_1(I_2)^2 + k_2 I_4 + 2k_3\chi I_3. \tag{6}$$

The spontaneous breaking results in the generation of hadron masses and the emergence of Nambu–Goldstone bosons [125]. To preserve scale invariance, in addition to scalar meson quartic self-interaction terms in $\mathcal{L}_0$, scale breaking terms are added, which are strategically scaled by glueball field χ [117]. Thus we obtain,

$$\begin{aligned}\mathcal{L}_0 = -\frac{1}{2}k_0\chi^2\left(\sigma^2 + \zeta^2 + \delta^2\right) + k_1\left(\sigma^2 + \zeta^2 + \delta^2\right)^2 \\ + k_2\left(\frac{\sigma^4}{2} + \frac{\delta^4}{2} + 3\sigma^2\delta^2 + \zeta^4\right) \\ + k_3\chi\left(\sigma^2 - \delta^2\right)\zeta - k_4\chi^4 - \frac{1}{4}\chi^4\ln\frac{\chi^4}{\chi_0^4} \\ + \frac{d}{3}\chi^4\ln\left(\left(\frac{\left(\sigma^2-\delta^2\right)\zeta}{\sigma_0^2\zeta_0}\right)\left(\frac{\chi}{\chi_0}\right)^3\right),\end{aligned} \tag{7}$$

Here, the last two terms account for scale-breaking potential in the model. In QCD, the trace of the energy–momentum tensor is not zero due to quantum effects, even in the massless limit. To emulate the trace anomaly of QCD, expressed as

$$\theta^{\mu}_{\mu} = \frac{\beta_{QCD}}{2g} G^{a}_{\mu\nu} G^{\mu\nu}_{a}. \tag{8}$$

Schechter [126] introduced the dilaton field originally within an effective Lagrangian framework at the tree level. In the above equation, $G^{a}_{\mu\nu}$ is the gluon field strength tensor, and $\beta(g)$ is the QCD beta function. The logarithmic terms have two primary effects: it breaks scale invariance, leading to the relationship $\theta^{\mu}_{\mu} \sim \chi^4$, and it induces a non-zero vacuum expectation value for the dilaton field, which in turn causes spontaneous chiral symmetry breaking [117]. By comparing the trace anomaly in QCD with that in the effective theory, the χ field can be identified with the gluon condensate as

$$\theta^{\mu}_{\mu} = \left\langle \frac{\beta_{QCD}}{2g} G^{a}_{\mu\nu} G^{\mu\nu}_{a} \right\rangle \propto (1-d)\chi^4. \tag{9}$$

The explicit chiral symmetry breaking is incorporated in the total Lagrangian by the term $\mathcal{L}_{\rm esb}$. The amalgamation of both spontaneous and explicit chiral symmetry-breaking components is crucial to comprehensively understand the mass spectrum and dynamics of hadrons within the QCD framework [127–129]. Mathematically, explicit symmetry breaking term is expressed as

$$\mathcal{L}_{\rm esb} = -\left(\frac{\chi}{\chi_0}\right)^2 \left[m_\pi^2 f_\pi \sigma + \left(\sqrt{2} m_K^2 f_K - \frac{1}{\sqrt{2}} m_\pi^2 f_\pi\right) \zeta \right]. \tag{10}$$

Using the effective Lagrangian of the chiral model, the thermodynamic potential (Ω) of the hadronic system can be expressed in terms of partition function ($\mathcal{Z}$) and temperature (T) as [123,130]

$$\Omega(T, V, \mu) = -T \ln \mathcal{Z}, \tag{11}$$

which gives

$$\begin{aligned} \frac{\Omega(T,V,\mu)}{V} = & -\frac{T}{(2\pi)^3} \sum_i \gamma_i \\ & \times \int d^3p \left\{ \ln\left(1 + e^{-\beta[E_i^*(p) - \mu_i^*]}\right) \right. \\ & \left. + \ln\left(1 + e^{-\beta[E_i^*(p) + \mu_i^*]}\right) \right\} \\ & - \mathcal{L}_{\rm vec} - \mathcal{L}_0 - \mathcal{L}_{\rm esb} - \mathcal{V}_{\rm vac}, \end{aligned} \tag{12}$$

with $E_i^*(k) = \sqrt{p^2 + m_i^{*2}}$ is the effective single particle energy and γ_i is the spin degeneracy factor. To obtain the vanishing value of vacuum energy, the potential energy ($\mathcal{V}_{\rm vac}$) is subtracted from the thermodynamic potential density.

2.2 Charged and uncharged baryons in the magnetic field

The total effective Lagrangian defined in Eq. (1) of the chiral model is modified to include an additional term contributing to the effects of an external magnetic field and is given by [131]

$$\mathcal{L}_{\rm total} = \mathcal{L}_{\rm chiral} + \mathcal{L}_{\rm mag}, \tag{13}$$

where

$$\mathcal{L}_{\rm mag} = -\bar{\psi}_i q_i \gamma_\mu A^\mu \psi_i - \frac{1}{4} \kappa_i \mu_N \bar{\psi}_i \sigma^{\mu\nu} F_{\mu\nu} \psi_i - \frac{1}{4} F^{\mu\nu} F_{\mu\nu}. \tag{14}$$

Here, ψ_i represents the wave function of the ith baryon, and the second term corresponds to the tensorial interaction involving the electromagnetic field tensor, denoted as $F_{\mu\nu}$. This term specifically characterizes the anomalous magnetic moment (AMM) and incorporates the parameter μ_N, which signifies the nuclear magneton. Since a uniform magnetic field is considered along the z-axis, the vector potential can be expressed as $A^\mu = (0, 0, Bx, 0)$. As a result, the Lorentz force comes into the picture, leading to quantized discrete Landau energy levels for charged particles moving in the field. Due to the interaction of baryons with the magnetic field, the momentum is divided into parallel ($p^i_\parallel$) and perpendicular ($p^i_\perp$) components. Thus, the integral in Eq. (12) is modified as

$$\int d^3p \to \frac{|q_i|\, B}{(2\pi)^2} \sum_n \int_{-\infty}^{\infty} dp^i_\parallel, \tag{15}$$

Also, the effective single-particle energy of charged baryons is altered in the magnetic field as [131,132]

$$\begin{aligned} \tilde{E}^i_{\nu,s} &= \sqrt{\left(p^i_\parallel\right)^2 + \bar{m_i}^2}, \quad \text{where,} \\ \bar{m_i} &= \left(\sqrt{m_i^{*2} + 2\nu|q_i|B} - s\mu_N \kappa_i B\right). \end{aligned} \tag{16}$$

In the above equation, the spin projection of the baryons in the direction of the magnetic field is given by $s = \pm 1$, and κ_i represents the anomalous magnetic moment of the baryons. Charged baryons with charge q_i, upon interaction with the magnetic field, undergo precessional motion within the transverse plane, described in terms of quantized Landau levels, $\nu = n + \frac{1}{2} - \frac{q_b}{|q_b|}\frac{s}{2} = 0, 1, 2, \ldots$. In the case of uncharged baryons, the transverse momentum is not defined

by the Landau levels, and the effective energy is defined as

$$\tilde{E}_s^i = \sqrt{\left(p_\parallel^i\right)^2 + \left(\sqrt{m_i^{*2} + \left(p_\perp^i\right)^2} - s\mu_N\kappa_i B\right)^2}. \quad (17)$$

By substituting the values of effective single-particle energy of charged and uncharged baryons in Eq. (12), as well as using the integral in Eq. (15) and minimizing the total thermodynamic potential density with respect to scalar and vector fields, the equation of motion under the influence of magnetic field is obtained for which the vector and scalar densities of charged baryons are identified as [133]

$$\rho_i^v = \frac{|q_i|B}{2\pi^2}\Bigg[\sum_{\nu=0}^{\nu_{max}^{(s=1)}}\int_0^\infty dp_\parallel^i\left(f_{p,\nu,s}^i - \bar{f}_{p,\nu,s}^i\right) + \sum_{\nu=1}^{\nu_{max}^{(s=-1)}}\int_0^\infty dp_\parallel^i\left(f_{p,\nu,s}^i - \bar{f}_{p,\nu,s}^i\right)\Bigg], \quad (18)$$

and

$$\begin{aligned}\rho_i^s = \frac{|q_i|Bm_i^*}{2\pi^2}\Bigg[&\sum_{\nu=0}^{\nu_{max}^{(s=1)}}\int_0^\infty \frac{dp_\parallel^i}{\sqrt{(p_\parallel^i)^2 + (\bar{m}_i)^2}} \\ &\times\left(1 - \frac{s\mu_N\kappa_i B}{\sqrt{m_i^{*2} + 2\nu|q_i|B}}\right)\left(f_{p,\nu,s}^i + \bar{f}_{p,\nu,s}^i\right) \\ &+ \sum_{\nu=1}^{\nu_{max}^{(s=-1)}}\int_0^\infty \frac{dp_\parallel^i}{\sqrt{(p_\parallel^i)^2 + (\bar{m}_i)^2}} \\ &\times\left(1 - \frac{s\mu_N\kappa_i B}{\sqrt{m_i^{*2} + 2\nu|q_i|B}}\right) \\ &\times\left(f_{p,\nu,s}^i + \bar{f}_{p,\nu,s}^i\right)\Bigg]. \end{aligned} \quad (19)$$

In the above equation, ν_{max} represents the maximum value of the Landau level [47]. Similarly, for uncharged baryons, we have

$$\rho_i^v = \frac{1}{2\pi^2}\sum_{s=\pm1}\int_0^\infty p_\perp^i dp_\perp^i \int_0^\infty dp_\parallel^i\left(f_{p,s}^i - \bar{f}_{p,s}^i\right), \quad (20)$$

and

$$\begin{aligned}\rho_i^s = \frac{1}{2\pi^2}\sum_{s=\pm1}\int_0^\infty p_\perp^i dp_\perp^i &\left(1 - \frac{s\mu_N\kappa_i B}{\sqrt{m_i^{*2} + \left(p_\perp^i\right)^2}}\right) \\ &\times\int_0^\infty dp_\parallel^i \frac{m_i^*}{\tilde{E}_s^i}\left(f_{p,s}^i + \bar{f}_{p,s}^i\right). \end{aligned} \quad (21)$$

In Eqs. (18) to (21), $f_{p,\nu,s}^i$, $\bar{f}_{p,\nu,s}^i$, $f_{p,s}^i$ and $\bar{f}_{p,s}^i$ denotes the Fermi distribution functions at finite temperature for particles and antiparticles, pertaining to both charged and uncharged baryons [131].

2.3 In-medium mass of kaons, ϕ and decay width of ϕ meson

The interactions within the chiral SU(3) model influence the in-medium masses of kaons and antikaons [84,85]. These interactions are described by the vector fields (ω, ρ, and ϕ) along with scalar fields (σ, ζ, and δ) and collectively contribute to the medium modification of energies for K and $\bar{K}$ mesons. Here, $K = \begin{pmatrix} K^+ \\ K^0 \end{pmatrix}$, and $\bar{K} = \begin{pmatrix} K^- & \overline{K}^0 \end{pmatrix}$ denote the isospin doublets of kaons and antikaons. Consequently, deriving dispersion relations for these particles necessitates accounting for isospin asymmetry stemming from the vector-isovector ρ field and the scalar-isovector δ field. The Lagrangian density describing the interactions of kaons with baryons in the strange asymmetric matter is given by [134–136]

$$\begin{aligned}\mathcal{L}_{KB} = -\frac{i}{4f_K^2}\Bigg[&\Big(2\bar{p}\gamma^\mu p + \bar{n}\gamma^\mu n - \bar{\Sigma^-}\gamma^\mu\Sigma^- + \bar{\Sigma^+}\gamma^\mu\Sigma^+ \\ &- 2\bar{\Xi^-}\gamma^\mu\Xi^- - \bar{\Xi^0}\gamma^\mu\Xi^0\Big) \\ &\times\Big(K^-(\partial_\mu K^+) - (\partial_\mu K^-)K^+\Big) \\ &+\Big(\bar{p}\gamma^\mu p + 2\bar{n}\gamma^\mu n + \bar{\Sigma^-}\gamma^\mu\Sigma^- \\ &- \bar{\Sigma^+}\gamma^\mu\Sigma^+ - \bar{\Xi^-}\gamma^\mu\Xi^- - 2\bar{\Xi^0}\gamma^\mu\Xi^0\Big) \\ &\times\Big(\bar{K^0}(\partial_\mu K^0) - (\partial_\mu\bar{K^0})K^0\Big)\Bigg] \\ &+\frac{m_K^2}{2f_K}\Bigg[(\sigma + \sqrt{2}\zeta + \delta)(K^+K^-) \\ &+(\sigma + \sqrt{2}\zeta - \delta)(K^0\bar{K^0})\Bigg] \\ &-\frac{1}{f_K}\Bigg[(\sigma + \sqrt{2}\zeta + \delta)(\partial_\mu K^+)(\partial^\mu K^-) \\ &+(\sigma + \sqrt{2}\zeta - \delta)(\partial_\mu K^0)(\partial^\mu\bar{K^0})\Bigg] \\ &+\frac{d_1}{2f_K^2}(\bar{p}p + \bar{n}n + \bar{\Lambda^0}\Lambda^0 + \bar{\Sigma^+}\Sigma^+ + \bar{\Sigma^0}\Sigma^0 \\ &+\bar{\Sigma^-}\Sigma^- + \bar{\Xi^-}\Xi^- + \bar{\Xi^0}\Xi^0) \\ &\times\Big((\partial_\mu K^+)(\partial^\mu K^-) + (\partial_\mu K^0)(\partial^\mu\bar{K^0})\Big) \\ &+\frac{d_2}{2f_K^2}\Bigg[(\bar{p}p + \frac{5}{6}\bar{\Lambda^0}\Lambda^0 + \frac{1}{2}\bar{\Sigma^0}\Sigma^0 + \bar{\Sigma^+}\Sigma^+ \\ &+\bar{\Xi^-}\Xi^- + \bar{\Xi^0}\Xi^0)(\partial_\mu K^+)(\partial^\mu K^-) \end{aligned}$$

$$+\left(\bar{n}n+\frac{5}{6}\bar{\Lambda^0}\Lambda^0+\frac{1}{2}\bar{\Sigma^0}\Sigma^0 +\bar{\Sigma^-}\Sigma^-+\bar{\Xi^-}\Xi^-+\bar{\Xi^0}\Xi^0\right)(\partial_\mu K^0)(\partial^\mu \bar{K^0})\Big]. \tag{22}$$

The first term in the above Lagrangian represents the vector interaction, commonly known as the Weinberg-Tomozawa term, and is derived from the kinetic part of the Lagrangian. The subsequent two terms emerge from explicit symmetry breaking, and the kinetic terms associated with pseudoscalars within the chiral effective Lagrangian [77]. The fourth and fifth terms are known as range terms that illustrate the interaction of mesons and baryons within the chiral effective model. The parameters d_1 and d_2 were determined from the empirical values of the KN scattering lengths for the $I=0$ and $I=1$ channels as $2.56/m_K$ and $0.73/m_K$, respectively [137,138]. By using the Fourier transformation of the equation of motion obtained using the KB interaction Lagrangian in Eq. (22), the dispersion relation of kaons and antikaons is written as [139]

$$-\omega^2+\vec{k}^2+m^2_{K(\bar{K})}-\Pi^*(\omega,\vec{k})=0, \tag{23}$$

where Π^* represents the medium-modified self-energy of kaons and antikaons [134]. For kaons, it is expressed as

$$\begin{aligned}\Pi^*_K(\omega,|\vec{k}|) = &-\frac{1}{4f_K^2}\Big[3(\rho_p^v+\rho_n^v)\pm(\rho_p^v-\rho_n^v)\pm 2(\rho_{\Sigma^+}^v-\rho_{\Sigma^-}^v)\\ &-\left(3(\rho_{\Xi^-}^v+\rho_{\Xi^0}^v)\pm(\rho_{\Xi^-}^v-\rho_{\Xi^0}^v)\right)\Big]\omega\\ &+\frac{m_K^2}{2f_K}(\sigma'+\sqrt{2}\zeta'\pm\delta')\\ &+\Big[-\frac{1}{f_K}(\sigma'+\sqrt{2}\zeta'\pm\delta')\\ &+\frac{d_1}{2f_K^2}(\rho_p^s+\rho_n^s+\rho^s{}_{\Lambda^0}+\rho^s{}_{\Sigma^+}\\ &+\rho^s{}_{\Sigma^0}+\rho^s{}_{\Sigma^-}+\rho^s{}_{\Xi^-}+\rho^s{}_{\Xi^0})\\ &+\frac{d_2}{4f_K^2}\Big((\rho^s{}_p+\rho^s{}_n)\pm(\rho^s{}_p-\rho^s{}_n)+\rho^s{}_{\Sigma^0}\\ &+\frac{5}{3}\rho^s{}_{\Lambda^0}+(\rho^s{}_{\Sigma^+}+\rho^s{}_{\Sigma^-})\pm(\rho^s{}_{\Sigma^+}-\rho^s{}_{\Sigma^-})\\ &+2\rho^s{}_{\Xi^-}+2\rho^s{}_{\Xi^0}\Big)\Big](\omega^2-\vec{k}^2),\end{aligned} \tag{24}$$

where the $\pm$ signifies the self-energy for K^+ and K^0 respectively. In the aforementioned expression, the terms σ', ζ', and δ' represent the deviations of the field expectation values from their respective vacuum expectation values. Similarly, the in-medium self-energy for antikaons is written as

$$\begin{aligned}\Pi^*_{\bar{K}}(\omega,|\vec{k}|)=&\frac{1}{4f_K^2}\Big[3(\rho_p^v+\rho_n^v)\pm(\rho_p^v-\rho_n^v)\pm 2(\rho_{\Sigma^+}^v-\rho_{\Sigma^-}^v)\\ &-\left(3(\rho_{\Xi^-}^v+\rho_{\Xi^0}^v)\pm(\rho_{\Xi^-}^v-\rho_{\Xi^0}^v)\right)\Big]\omega\\ &+\frac{m_K^2}{2f_K}(\sigma'+\sqrt{2}\zeta'\pm\delta')\\ &+\Big[-\frac{1}{f_K}(\sigma'+\sqrt{2}\zeta'\pm\delta')\\ &+\frac{d_1}{2f_K^2}(\rho_p^s+\rho_n^s+\rho^s{}_{\Lambda^0}+\rho^s{}_{\Sigma^+}\\ &+\rho^s{}_{\Sigma^0}+\rho^s{}_{\Sigma^-}+\rho^s{}_{\Xi^-}+\rho^s{}_{\Xi^0})\\ &+\frac{d_2}{4f_K^2}\Big((\rho^s{}_p+\rho^s{}_n)\pm(\rho^s{}_p-\rho^s{}_n)+\rho^s{}_{\Sigma^0}\\ &+\frac{5}{3}\rho^s{}_{\Lambda^0}+(\rho^s{}_{\Sigma^+}+\rho^s{}_{\Sigma^-})\pm(\rho^s{}_{\Sigma^+}-\rho^s{}_{\Sigma^-})\\ &+2\rho^s{}_{\Xi^-}+2\rho^s{}_{\Xi^0}\Big)\Big](\omega^2-\vec{k}^2),\end{aligned} \tag{25}$$

with $\pm$ symbol depicting K^- and $\bar{K^0}$ respectively. The terms m_K and $m_{\bar{K}}$ in the above equations represent the vacuum mass value of kaon and antikaon. By solving Eq. (23) at $|\vec{k}|=0$, the in-medium masses of kaons and antikaons (which is known as pole mass) are obtained in the asymmetric strange matter under the influence of the external magnetic field. However, due to the presence of the external magnetic field, the effective mass of the charged K^+ and K^- gets additionally modified due to Landau quantization as [116]

$$m^{eff}_{K^\pm}=\sqrt{(m^*_{K^\pm})^2+|qB|} \tag{26}$$

The contribution from the lowest Landau level (LLL) is considered for the calculation of masses of kaons and antikaons in the medium, as given by Eq. (26). In the current study, the effect of magnetic field on kaons and antikaons effective masses has been studied by considering the effect of anomalous magnetic moment (AMM) of the hadrons. In Ref. [108], the effects of the anomalous magnetic moment (AMM) of protons and neutrons were considered, and the required number of Landau levels contributing at different values of $|eB|$ at ρ_0 were analyzed. It was found that at $|eB|=1m_\pi^2$, the maximum Landau level contributions were $\nu^{up}_{max}=2$ and $\nu^{down}_{max}=1$, corresponding to the spin-up and spin-down projections of protons along the field axis. As the magnetic field increased to $|eB|=2m_\pi^2$, the contributing levels reduced to $\nu^{up}_{max}=0$ and $\nu^{down}_{max}=1$. For magnetic fields stronger than $|eB|>2m_\pi^2$, only the $\nu=0$ Landau level contributed. The systematic reduction in the number of contributing Landau levels with increasing magnetic field strength supports the validity

of the LLL approximation at both finite density and vacuum. This widely-used approach exploits the separation between the LLL and higher Landau levels (HLLs) by neglecting the contributions from all higher levels, considering only those from the LLL, as in Refs. [140–144].

By solving the dispersion relation given by Eq. (23), we calculate the in-medium masses of kaons and antikaons at zero momentum ($\vec{k} = 0$), for finite density and temperature of the medium. The study of screening mass, which corresponds to condition $\omega = 0$, is also important for studies at finite temperature [145]. In Ref. [146], it is demonstrated that the screening mass of kaons remains constant as a function of temperature for T $<$ 150 MeV and increases monotonically at higher temperatures. For $\omega = 0$, the dispersion relation in Eq. (23) simplifies to, $\vec{k}^2 + m^2_{K(\bar{K})} - \Pi^*(0, \vec{k}) = 0$. The screening mass $m_{\text{screening}}$ is related to the static limit of the dispersion relation and can be determined by solving $m^2_{\text{screening}} = m^2_{K(\bar{K})} - \Pi^*(0, \vec{k} = im_{\text{screening}})$ [147]. This shows that the screening mass is derived from the modified dispersion relation in the static limit, indicating how the effective mass of the kaon in a medium influences the spatial decay of its interactions. The spatial behavior of kaons in the medium is an important aspect and can be studied in future work. This will allow us to study screening effects explicitly and provide a more detailed understanding of the medium's impact on both the temporal and spatial directions.

To study the properties of ϕ meson in finite magnetic field, the in-medium masses of kaons are utilized to evaluate the self-energy of the ϕ meson concerning the decay process $\phi \to K\bar{K}$ at the one-loop level [67,85,148]. The interaction Lagrangian for this process is defined as

$$\mathcal{L}_{\phi K \bar{K}} = i g_\phi \phi^\mu \left[\bar{K}(\partial_\mu K) - (\partial_\mu \bar{K})K\right], \tag{27}$$

where g_ϕ is the coupling constant. The interactions represented by $\phi\phi K\bar{K}$ are neglected in the current study due to a trivial contribution to medium masses and decay width [85]. The scalar part of the medium modified self-energy in the rest frame of ϕ meson, which is derived from the one loop diagram, is formulated as [84,85]

$$i\Pi^*_\phi(p) = -\frac{8}{3} g^2_\phi \int \frac{d^4q}{(2\pi)^4} \vec{q}^{\,2} D_K(q) D_{\bar{K}}(q - p), \tag{28}$$

where the kaon propagator is given by

$$D_K(q) = \left(q^2 - m^{*^2}_K + i\epsilon\right)^{-1}, \tag{29}$$

and antikaon propagator as

$$D_{\bar{K}}(q - p) = \left((q - p)^2 - m^{*^2}_{\bar{K}} + i\epsilon\right)^{-1}. \tag{30}$$

In the above equation, the four-momentum vector for ϕ meson is written as $p = (p^0 = m^*_\phi, \vec{0})$ where, m^*_ϕ signifies the in-medium ϕ meson mass. The m^*_K and $m^*_{\bar{K}}$ in Eqs. (29) and (30), depicts the mass average of the kaon doublet, (K^+, K^0) and antikaon doublet, (K^-, $\bar{K}^0$), respectively. The value of coupling constant g_ϕ comes out to be 4.539, derived from the observed width of the ϕ meson in a vacuum. This coupling constant alongside the vacuum mass of the ϕ meson, which is considered to be 1019.461 MeV, is used to determine the bare mass of the ϕ meson [149]. The real part of Eq. (28) is solved to obtain the in-medium mass of ϕ meson as

$$m^{*^2}_\phi = \left(m^0_\phi\right)^2 + \Re\Pi^*_\phi(m^{*^2}_\phi), \tag{31}$$

where m^0_ϕ is the bare mass of the ϕ meson. While solving the Eq. (31), the integral within the real part of the self-energy for the ϕ meson is divergent. Hence, to prevent encountering singularities, we regularize the integral by employing a phenomenological form factor by incorporating a cutoff parameter, Λ_c [150]. After regularization, we obtain

$$\Re\Pi^*_\phi = -\frac{4}{3} g^2_\phi \mathcal{P} \int_0^{\Lambda_c} \frac{d^3q}{(2\pi)^3} \vec{q}^{\,4} \times \left(\frac{\Lambda_c^2 + m^{*^2}_\phi}{\Lambda_c^2 + 4E^{*^2}_K}\right)^4 \frac{(E^*_K + E^*_{\bar{K}})}{E^*_K E^*_{\bar{K}}((E^*_K + E^*_{\bar{K}})^2 - m^{*^2}_\phi)}. \tag{32}$$

The cutoff parameter in the above equation is calculated by comparing the root mean square radii, which are calculated using two distinct form factors, resulting in an expression for Λ_c in relation to oscillator constants, β_D and β_Ψ. This method has been used to determine Λ_c in the studies of J/Ψ and D mesons [150,151]. The decay width of ϕ meson is determined from the imaginary part of the self-energy and given by the expression as [81]

$$\Gamma^*_\phi = \frac{g^2_\phi}{24\pi} \frac{1}{m^{*^5}_\phi} \left((m^{*^2}_\phi - (m^*_K + m^*_{\bar{K}})^2) \times (m^{*^2}_\phi - (m^*_K - m^*_{\bar{K}})^2)\right)^{3/2}. \tag{33}$$

Thus, using the in-medium masses of kaons and antikaons derived from the self-energy expression in Eqs. (24) and (25), the effective mass and decay width of ϕ is calculated in the presence of an external magnetic field. Note that to calculate the decay width of ϕ mesons in the present calculations we considered the contributions through the medium modified masses only. At finite temperatures, particles acquire a thermal width because of increased interactions with the surrounding medium, including scattering processes. Models like chiral perturbation theory [152], linear sigma model

[153], one-boson-exchange model [154], and QCD sum rules [155] demonstrate that particles such as pions and nucleons develop a thermal width that increases with temperature, indicating a higher interaction rate in hot and dense environments. The effect of thermal width becomes dominant for ρ and $a_1(1260)$ meson essentially for $T/T_c > 0.7$, where T_c is the critical temperature for deconfinement [153,155]. The collision broadening of ϕ mesons with the baryons of the medium has been studied in [156] and leads to broadening of Γ_ϕ by $\sim$ 10 MeV at 170 MeV. In Ref. [157], contribution to decay width of ϕ mesons due to collision broadening by ρ mesons is investigated. The impact of collision rates of ϕ mesons with ρ, K and K^* mesons has also been studied in Ref. [158]. Impact of such interactions on the total decay width will be considered in the future work.

3 Results and discussion

In this section, the results obtained for medium modification of K, $\bar{K}$, and ϕ meson masses in the asymmetric strange magnetized hadronic matter have been discussed in detail. The change in the mass of kaons and antikaons arises due to their interactions with the baryon octet. The charged K^+ and K^- mesons undergo an additional mass modification due to an external magnetic field, whereas the neutral K^0 and $\bar{K}^0$ have comparatively negligible changes due to magnetic field. To derive this mass modification of K and $\bar{K}$ in the presence of a magnetic field, the scalar and vector fields are solved from equations of motion obtained by minimizing the thermodynamic potential density. The effective mass and decay width of ϕ meson have been calculated from in-medium mass modification of kaons and antikaons.

In the present work, the parameters k_0, k_2, and k_4 governing the scalar self-interactions of the fields σ, ζ, and χ are fitted by minimizing the thermodynamic potential density in the vacuum, accurately representing the spontaneous breaking of chiral symmetry. The parameter k_1 is set to match the vacuum mass of the σ meson, while k_3 is calibrated to reproduce the mass splitting between the η and η' mesons [122]. Additionally, the scalar coupling constants are adjusted within the model to obtain the vacuum masses of the baryon octet, and vector coupling constants are fit to reproduce nuclear saturation properties, binding energy, compressibility and symmetry energy [122]. The parameter d, which is related to scalar scale breaking, is determined from the one-loop QCD beta function. The vacuum value of χ_0 is chosen to ensure zero pressure at nuclear saturation density, whereas σ_0 and ζ_0 are fitted to the decay constants of the π and K mesons, respectively. The model parameters in the current work are given in Table 1. The isospin asymmetry of the medium accounting for unequal densities of isospin multiplets is represented in terms of parameter, $I_a = -\frac{\Sigma_i \tau_{3i} \rho_i^v}{2\rho_B}$, where, ρ_B, is the total baryonic density. To consider the relative abundance of strange baryons within the hadronic system under investigation, it is characterized by the strangeness fraction parameter denoted as $f_s = \frac{\Sigma_i |s_i| \rho_i^v}{\rho_B}$, where s_i is the strangeness number of the i^{th} particle.

In Figs. 1, 2 and 3, the variation of K and $\bar{K}$ masses have been shown as a function of varying magnetic field at baryonic densities, $\rho_B = 0$, ρ_0 and $2\rho_0$ and temperature values, $T = 0$, 100 and 150 MeV, respectively. The value of baryonic density is set to low values to consider the conditions of heavy-ion collisions like LHC and RHIC, where the magnetic field is anticipated in low-density regimes [96]. The in-medium masses have been depicted for $f_s = 0$ and 0.3 and isospin asymmetry parameter, $I_a = 0$ and 0.3. The effective masses of kaons and antikaons are determined from the dispersion relation in Eq. (23), incorporating additional positive shifts for the charged mesons as defined in Eq. (26). These shifts result from the direct interaction of these mesons with the magnetic field through minimal coupling. The vectorial Weinberg–Tomozawa term, the first term in self-energy of kaons and antikaons in Eqs. (24) and (25) induces a rise in mass for kaons and a drop in the mass for antikaons as a function of density at zero magnetic field strength. In this scenario, the second term, referred to as the scalar exchange term, is attractive for both kaons and antikaons. The last three

Table 1 Parameters used in the present work

k_0	k_1	k_2	k_3	k_4	σ_0 (MeV)	ζ_0 (MeV)
2.53	1.35	− 4.77	− 2.77	− 0.21	− 93.3	− 106.763
δ_0	χ_0	ρ_0 (fm^{-3})	$g_{\sigma N}$	$g_{\zeta N}$	$g_{\delta N}$	$g_{\omega N}$
0	409.76	0.15	10.6	− 0.46	2.48	13.32
$g_{\rho N}$	$g_{\sigma \Lambda}$	$g_{\zeta \Lambda}$	$g_{\delta \Lambda}$	g_4	d	$g_{\sigma \Sigma}$
5.48	7.52	5.80	0	79.81	0.064	6.13
$g_{\zeta \Sigma}$	$g_{\delta \Sigma}$	f_π (MeV)	f_K (MeV)	$g_{\sigma \Xi}$	$g_{\zeta \Xi}$	$g_{\delta \Xi}$
5.80	6.79	93.3	122.143	3.78	9.14	2.36
m_π (MeV)	m_K (MeV)	m_N (MeV)				
139	498	939				

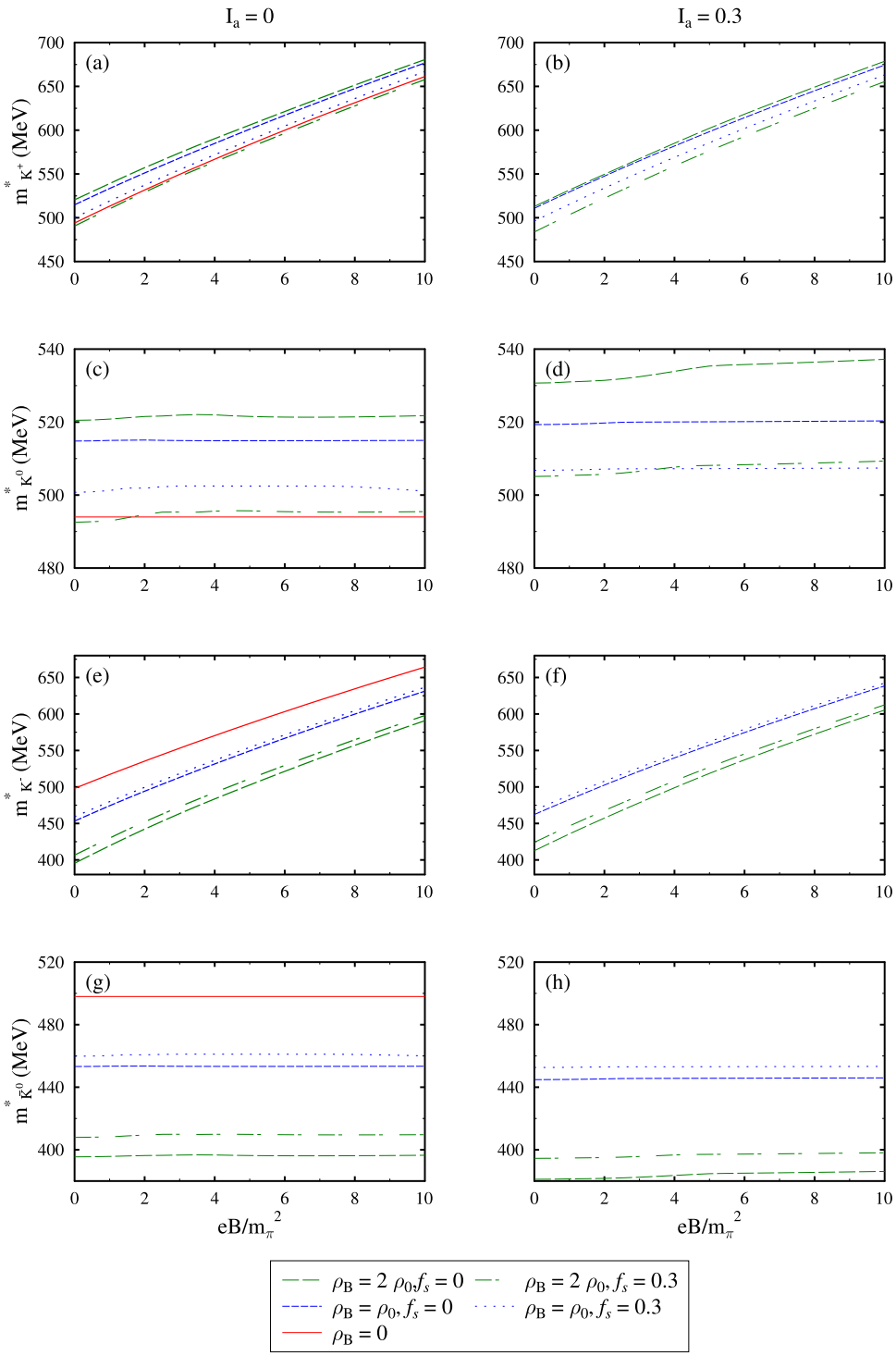

Fig. 1 The masses of K and $\bar{K}$ have been plotted as a function of magnetic field for baryonic densities, $\rho_B = 0$, ρ_0 and $2\rho_0$ at temperature, $T = 0$. Plots have been shown for varying values of strangeness fraction, f_s, and isospin asymmetry parameter, I_a

terms in the self-energy account for range effects. The first term is repulsive, whereas the second and third range terms (designated as d_1 and d_2) are attractive for both kaons and antikaons.

In isospin-symmetric matter represented by $I_a = 0$, the value of the scalar-isovector meson field, δ, and vector isovector meson field, ρ, remains zero for the vanishing value of the magnetic field. Thus, the isospin doublet pairs, K^+ and K^0, K^- and $\bar{K}^0$, have equal masses for all densities and temperatures. But in asymmetric matter, the masses of isospin doublets undergo changes due to the non-zero contribution of δ fields. For $eB = 0$, $T = 0$ and $I_a = 0.3$, K^+ mass decreases by 0.36% whereas K^0 mass increases by 0.43% in non-strange medium at saturation density. Due to the non-zero value of δ and ρ fields for finite I_a, the effective mass of the K^+ meson derived from Eq. (24) is predominantly influ-

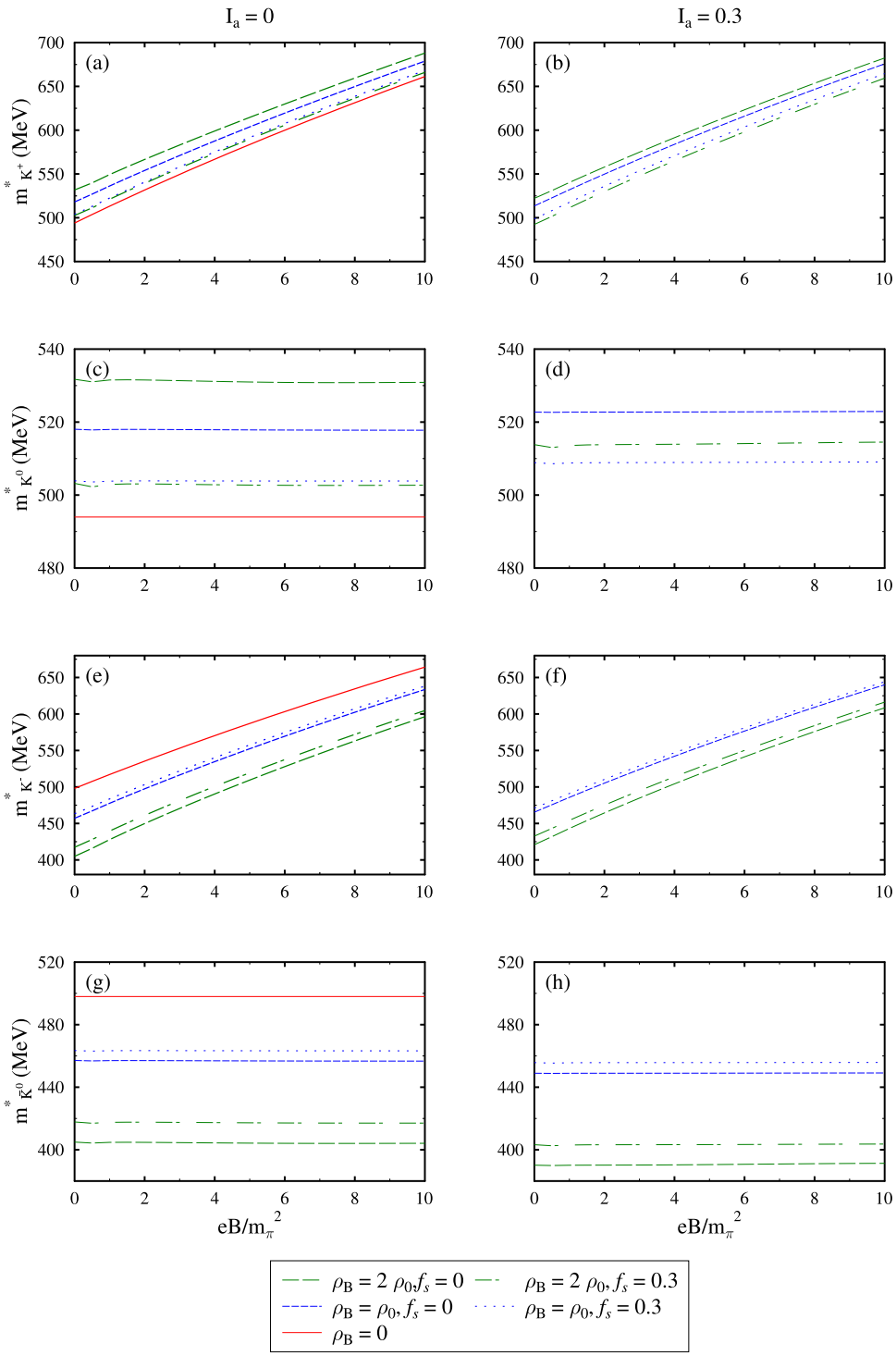

Fig. 2 The masses of K and $\bar{K}$ have been plotted as a function of magnetic field for baryonic densities, $\rho_B = 0$, ρ_0 and $2\rho_0$ at temperature, $T = 100$ MeV. Plots have been shown for varying values of strangeness fraction, f_s, and isospin asymmetry parameter, I_a

enced by the scalar and vector densities of baryons with a positive τ_3 value. Conversely, the self-energy of the K^0 meson is primarily dictated by the densities of baryons with a negative τ_3 value in Eq. (24). Consequently, the Weinberg–Tomozawa term tends to be more repulsive for K^0 mesons, thus suppressing the attractive contributions from the d_2 range term. In case of $\bar{K}$ isospin doublet, as the isospin asymmetry is increased from 0 to 0.3, the effective mass of $K^-(\bar{K^0})$ increases (decreases) by 2.29%(2.09%). Note that the opposite behavior of K^+ and K^- meson masses for increased isospin asymmetry is because of Weinberg Tomozawa term which contribute with opposite sign for K and $\bar{K}$ mesons (see the sign of first term in Eqs. (24) and (25)). Thus, the mass of K^+ decreases while that of K^- increases for an increase in the isospin asymmetry I_a, at given density and magnetic field.

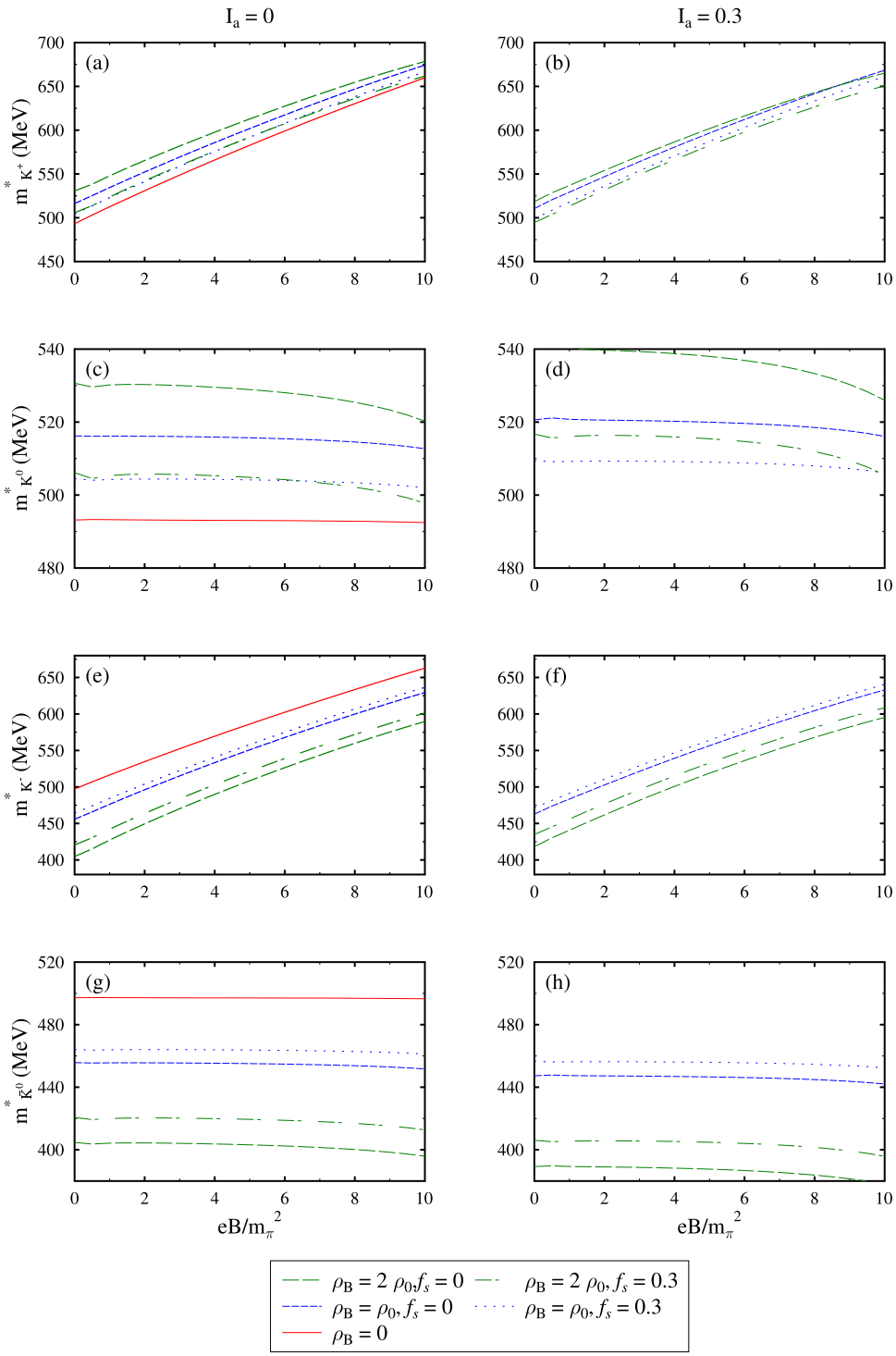

Fig. 3 The masses of K and $\bar{K}$ have been plotted as a function of magnetic field for baryonic densities, $\rho_B = 0$, ρ_0 and $2\rho_0$ at temperature, $T = 150$ MeV. Plots have been shown for varying values of strangeness fraction, f_s, and isospin asymmetry parameter, I_a

Transitioning from a nonstrange to a strange medium, the mass of the K^+ and K^0 meson experiences a decrement. This trend arises because the range term d_1 becomes more negative in transitioning to a strange medium while the d_2 term becomes less negative. As a result, the attractive nature of the d_1 term prevails over the range terms, leading to an overall decrease in the masses of both K^+ and K^0 mesons within the strange medium as a function of density. Whereas due to the attractive contribution of vectorial term, the masses of K^- and $\bar{K}^0$ increase in the strange matter as the density value increases for a given magnetic field value. In the case of the finite magnetic field, the mass of charged kaons (K^+ and K^-) is modified due to their direct interaction with the magnetic field, whereas, for electrically neutral mesons (K^0 and $\bar{K}^0$), there is no corresponding mass modification for $\rho_B = 0$. The interaction of the nucleons and hyperons

with the magnetic field leads to a nonzero value for the δ field for all density values, indicating that isospin symmetry is broken despite I_a=0. The masses of the K^0 and $\bar{K}^0$ are impacted due to the change in density, the strangeness fraction, and the asymmetry of the system. At nuclear saturation density, the masses of K^+ and K^- have been shown to rise by 32% and 39% when eB/m_π^2 is changed from 0 to 10 in nuclear non-strange symmetric matter. The authors in Ref. [116] have reported an increment of 25% and 32% in the masses of K^+ and K^- for similar conditions in analysis of nuclear matter in the framework of the chiral hadronic model when eB/m_π^2 varies from 2 to 8. The masses of K and $\bar{K}$ show very little change with the rise in temperature value for a given density value. With the increase in the temperature value, there is an increase in masses of K and $\bar{K}$, but this is more evident at high-density values [84]. Using the quark meson coupling model in nonstrange symmetric nuclear matter at zero temperature, the authors in Ref. [85] observed that the mass of kaons decreases as a function of baryonic density. An increase in masses of kaons and decrease in masses of antikaons as a function of density has been observed in Ref. [81] by employing a relativistic transport model approach. As discussed earlier, the values of parameters d_1 and d_2 appearing in Eq. (22) are determined using the kaon-nucleon scattering length. If the value of d_1 and d_2 are increased by 10% in the non-strange isospin symmetric matter, there is a decrease in effective mass of K^+, K^0, K^- and $\bar{K}^0$ by 0.9%, 1.2%, 0.7% and 1.0%, respectively, at saturation density for $eB = 5m_\pi^2$ and temperature $T = 0$. On the contrary, for a decrement of 10% in values of d_1 and d_2, there is an increase in the effective mass of K^+ by 1.0%, K^0 by 1.3%, K^- by 0.8% and $\bar{K}^0$ by 1.1%.

Utilizing the in-medium masses of kaons and antikaons, it is possible to compute the in-medium optical potential for finite momentum conditions by using $U^*_{K(\bar{K})}(\omega, \vec{k}) = \omega(\vec{k}) - \sqrt{\vec{k}^2 + {m^*_{K(\bar{K})}}^2}$. In this expression, $\omega(\vec{k})$ represents

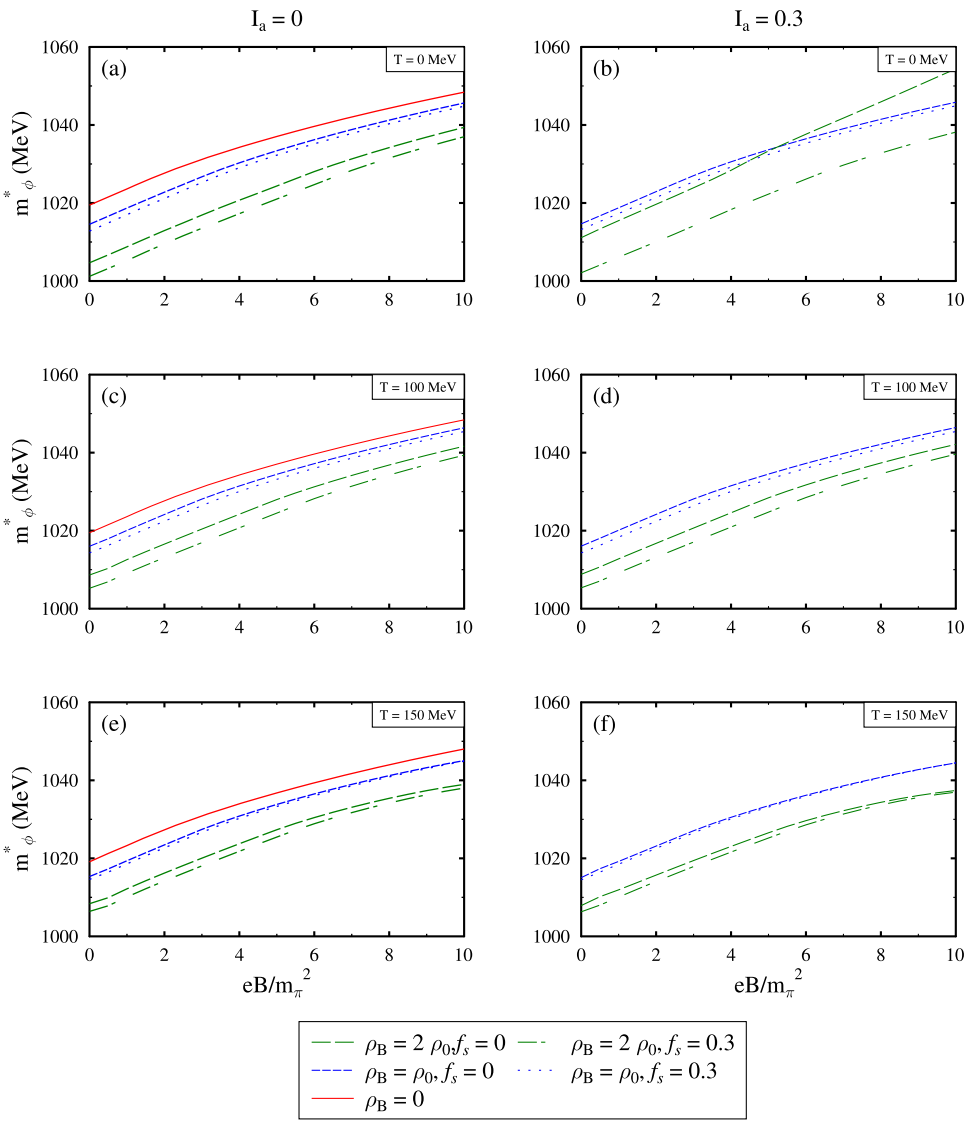

Fig. 4 The mass of ϕ meson has been plotted as a function of magnetic field for baryonic densities, $\rho_B = 0$, ρ_0 and $2\rho_0$ at temperature, $T = 0$, 100 and 150 MeV. Plots have been shown for varying values of strangeness fraction, f_s, and isospin asymmetry parameter, I_a

Table 2 The above table shows the values of the in-medium mass of ϕ meson (mass and T are expressed in the units of MeV)

	f_s	$eB/m_\pi^2 = 0$				$eB/m_\pi^2 = 5$				$eB/m_\pi^2 = 10$			
		I_a=0		I_a=0.3		I_a=0		I_a=0.3		I_a=0		I_a=0.3	
		ρ_0	$2\rho_0$	ρ_0	$2\rho_0$	ρ_0	$2\rho_0$	ρ_0	$2\rho_0$	ρ_0	$2\rho_0$	ρ_0	$2\rho_0$
$T = 0$	0	1014.5	1004.6	1014.6	1011.1	1033.3	1024.3	1033.6	1033.3	1045.6	1039.3	1045.8	1054.3
	0.3	1012.8	1001.1	1013.2	1002.1	1032.2	1021.0	1032.4	1022.2	1044.8	1036.9	1044.9	1038.1
$T = 100$	0	1015.9	1008.6	1016.0	1008.8	1034.4	1027.9	1034.5	1028.4	1046.3	1041.6	1046.4	1042.1
	0.3	1014.3	1005.2	1014.2	1005.3	1033.1	1024.4	1033.1	1024.7	1045.4	1039.3	1045.4	1039.6
$T = 150$	0	1015.3	1008.3	1015.0	1007.8	1033.8	1027.3	1033.4	1026.5	1045.0	1038.9	1044.4	1037.3
	0.3	1014.5	1006.3	1014.4	1006.2	1033.3	1025.4	1033.1	1025.2	1044.9	1038.0	1044.4	1036.9

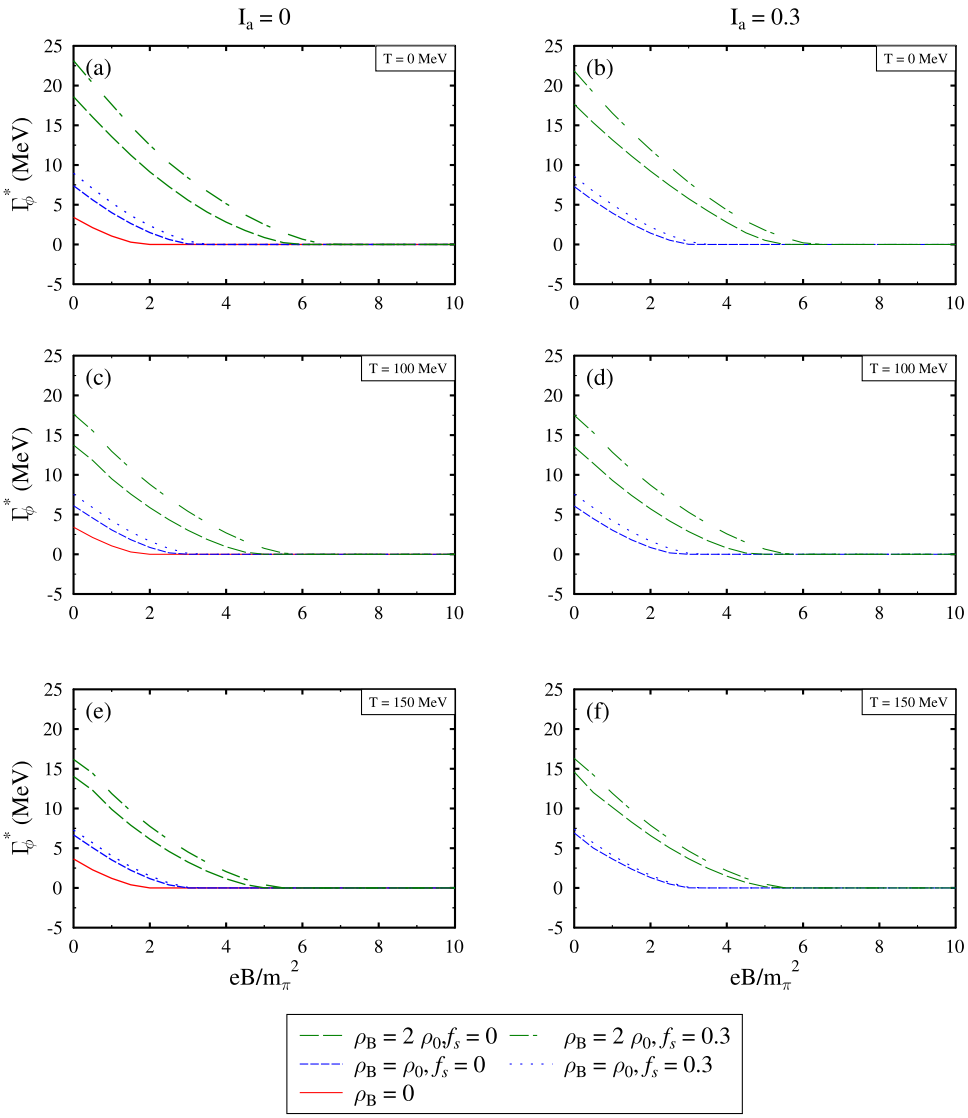

Fig. 5 The decay width of ϕ have been plotted as a function of magnetic field for baryonic densities, $\rho_B = 0$, ρ_0 and $2\rho_0$ at temperature, $T = 0$, 100 and 150 MeV. Plots have been shown for varying values of strangeness fraction, f_s, and isospin asymmetry parameter, I_a

the energy of the kaon or antikaon at momentum $\vec{k}$. In regimes of extremely low densities, where the impulse approximation holds $U \approx -4\pi a_{\bar{K}N}\rho$, the optical potential for antikaons will exhibit a positive value due to the repulsive nature of the scattering length at the $\bar{K}N$ threshold [159]. Initial efforts to derive the antikaon-nucleus potential from examining kaonic-atom data indicated notably potent attractive potentials, ranging from $-$ 150 to $-$ 200 MeV at the nuclear saturation density, ρ_0 [160]. The coupled-channel approach yields attractive potentials of range $-$ 50 to $-$ 80 MeV at ρ_0 for antikaons by incorporating medium effects via Pauli blocking and the self-consistent treatment of the antikaon's self-energy, a necessary aspect for explaining kaonic atom data [161,162]. However, the present study and other theoretical approaches to the in-medium characteristics of kaons and antikaons have relied on the mean-field approach. This method has also been utilized to explore the properties of K and $\bar{K}$ at high values of ρ_B, as demonstrated in previous works [84,85,139,163]. A slightly attractive potential for K^+ meson for densities lower than $2.5\rho_0$ has been predicted in the mean-field quark meson coupling model in Ref. [164]. Such investigations are relevant to the high baryonic density conditions that may be generated in the forthcoming compressed baryonic matter (CBM) experiment at the Facility for Antiproton and Ion Research (FAIR) in Darmstadt.

In our previous non-magnetic investigation of ϕ meson, the mass and decay width dependence on varying regularization parameter values has been studied in detail [84]. It has been reported that there is a decrease in the value of decay width with a change in Λ_c from 1 to 4 GeV. In Fig. 4, the effective mass of ϕ meson has been shown as a function of magnetic field for different temperature and density values for regularization parameter, $\Lambda_c = 3$ GeV. The mass modification of ϕ meson in the hadronic medium with varying magnetic field and temperature values are derived from in-medium masses of K and $\bar{K}$ and have been tabulated in Table 2 for different input parameter values. With an increase in the magnetic field, due to a constant increase in masses of K^+ and K^-, and negligible change in masses of K^0 and $\bar{K}^0$, as a result, there is a continuous rise in the mass of ϕ meson for all values of I_a and f_s. For low values of the density, there is a very negligible change in the masses of K and $\bar{K}$ with increasing temperature, and hence, the m^*_ϕ changes from 1014 MeV at $T = 0$ to 1015 MeV at $T = 150$ MeV for $\rho_B = \rho_0$ in case of non-strange symmetric matter at zero magnetic field strength.

From Table 2 we observe that, for a give baryon density ρ_B, at low temperature, the in-medium masses of ϕ mesons decreases slightly as a function of isospin asymmetry of the medium, whereas, at high T, there is observed to be a slight increase. This behaviour can be understood in terms of isospin dependence of scalar fields σ and ζ within the chiral SU(3) model. In the chiral SU(3) model, to calculate the in-medium properties of different mesons and baryons, one first solve the coupled system of equations for the scalar fields σ, ζ and δ and vector field ω, ρ and ϕ. The behaviour of in-medium masses of mesons is closely related to the values of scalar fields σ and ζ. For given isospin asymmetry of the medium, the magnitude of scalar fields decreases with an increase in the baryon density of the medium. On the other-hand, for given density and at low temperature, an increase the isospin asymmetry of the medium causes a slight increase in the magnitude of these scalar fields. However, as the temperature is increased, the impact of isospin asymmetry of the medium is decreased. This behaviour of scalar fields as a function of isospin asymmetry is reflected in the in-medium masses of ϕ mesons. By considering pseudoscalar and vector mesons mixing (PV mixing), a monotonous rise in the ϕ meson mass for increasing magnetic field values has also been observed in Ref. [165]. In the study of the mass modification of light vector mesons by applying the QCD sum rules approach, a negligible change with the magnetic field is noticed for ϕ meson [166–168]. However, with the change in density from ρ_0 to $4\rho_0$ at a fixed value of $eB/m_\pi^2 = 4$ in isospin asymmetric nuclear matter, a decrease of 0.42% in ϕ meson mass has been reported.

Figure 5 depicts the in-medium partial decay width (Γ^*_ϕ) as a function of the magnetic field for different temperature and density values. The decay width has been calculated by obtaining the imaginary part of the self-energy for the decay of ϕ meson into $K\bar{K}$ pair [169]. The in-medium value of the partial decay width of ϕ meson has been tabulated in Table 3. As the value of density increases from zero to $2\rho_0$, there is a rise in the value of the partial decay width of ϕ meson for all values of magnetic field and temperature. As the magnetic field strength increases, the masses of the charged kaons, (K^+ and K^-), also shows an increment. In the decay process $\phi \rightarrow K\bar{K}$, it is a fundamental requirement that the parent ϕ meson must have a mass greater than the combined masses of the decay products. Consequently, as the masses of the K and K^- increase with the magnetic field, the available phase space for the decay process diminishes. This reduction in phase space leads to a decreased probability of ϕ meson decay as the magnetic field strength increases, resulting in a suppression of the decay width under stronger magnetic fields. This behavior underscores the significant influence of the medium, particularly the magnetic field, on the decay dynamics of the ϕ meson.

A comparatively high decay width is observed in a shift from non-strange to strange medium for all density values in the magnetic and non-magnetic medium. This is attributed to the fact that there is a drop in mass of ϕ meson in the strange medium and increased density. For all values of I_a and f_s, the decay width ceases to be zero with increasing magnetic field and given value of density and temperature. As explained before, due to the increase in mass of K and $\bar{K}$ with increas-

Table 3 The above table shows the values of partial decay width of ϕ meson (decay width and T are expressed in the units of MeV)

	f_s	$eB/m_\pi^2 = 0$				$eB/m_\pi^2 = 5$				$eB/m_\pi^2 = 10$			
		$I_a = 0$		$I_a = 0.3$		$I_a = 0$		$I_a = 0.3$		$I_a = 0$		$I_a = 0.3$	
		ρ_0	$2\rho_0$	ρ_0	$2\rho_0$	ρ_0	$2\rho_0$	ρ_0	$2\rho_0$	ρ_0	$2\rho_0$	ρ_0	$2\rho_0$
$T = 0$	0	7.3	18.6	7.2	17.6	0	0.8	0	0.5	0	0	0	0
	0.3	8.9	23.1	8.5	21.8	0	2.5	0	1.7	0	0	0	0
$T = 100$	0	6.1	13.7	6.0	13.5	0	0	0	0	0	0	0	0
	0.3	7.5	17.6	7.5	17.5	0	0.7	0	0.6	0	0	0	0
$T = 150$	0	6.6	14.0	6.9	14.6	0	0	0	0.1	0	0	0	0
	0.3	7.2	16.1	7.3	16.3	0	0.4	0	0.4	0	0	0	0

ing magnetic field, after a certain value of eB, the collective masses of K and $\bar{K}$ is greater than the mass of ϕ meson. As the value of the mass of products becomes greater than the mass of the decaying particle, the decay width becomes zero. This signifies the zero probability of occurrence of such decay processes at a high magnetic field value. For a given value of temperature and magnetic field, with the increase in the value of density and the strangeness of the medium, the mass of ϕ meson decreases. Thus, the decay width increases as a function of density. Thus, the decay width value becomes zero at comparatively higher magnetic field values with increasing density. By employing a chiral mean-field model, complemented by a phenomenological $K - \phi$ interaction, a similar trend in the decay-width of ϕ meson with varying magnetic fields has been studied in Ref. [107]. In heavy-ion collision experiments, employing the decay width allows for measuring ϕ meson production in pN collisions [170,171]. Comparing experimental data with model predictions will provide insights into the production of ϕ mesons in the strange asymmetric hadronic matter.

4 Summary

In summary, the medium modification of K and $\bar{K}$ masses in asymmetric magnetized strange matter have been utilized to study the in-medium properties of ϕ meson. The medium modifications are considered by considering the interactions of scalar and vector fields in the framework of a mean-field effective chiral SU(3) model. The masses of kaons and antikaons are calculated by solving the interaction Lagrangian. These in-medium masses of K and $\bar{K}$ are further incorporated in the self-energy of ϕ meson by contemplating the one-loop level corrections in the decay process $\phi \rightarrow K\bar{K}$. By using the effective mass of ϕ meson, the partial decay width of the given process is calculated from the imaginary part of the self-energy. The temperature dependence of the K, $\bar{K}$, and ϕ in an external magnetic field is examined by analyzing the change in scalar and vector fields at varying density and temperature values. Due to the electromagnetic interaction and Landau quantization in the presence of an external magnetic field, a significant linear rise in charged K^+ and K^- masses is observed. Whereas the mass modifications in uncharged K^0 and $\bar{K}^0$ mesons are attributed to changes in density and temperature conditions. Due to these interactions, ϕ meson mass increases monotonously with increasing magnetic field. When the effective mass of ϕ meson becomes comparatively less than the decay products in the defined decay channel, the partial decay width becomes zero, resulting in Γ^*_ϕ becoming independent of applied magnetic field strength.

Our current investigation focuses on the ϕ self-energy within the medium, primarily attributing it to the modifications in the kaon-antikaon loop induced by the medium. The ϕ meson is critical in resolving the hyperon puzzle in neutron stars and magnetars [172,173]. Hyperons soften the hadronic equation of state at medium to high densities, reducing the maximum mass of neutron stars below observed values like the two solar mass PSR J1614-2230 [174]. The ϕ meson introduces additional repulsion in hyperon-hyperon interactions, potentially reconciling theoretical models with observations. Our findings suggest that the ϕ meson remains stable under high magnetic fields, confirming its role as a probe in high-energy hadronization processes. However, further exploration into the role of gluonic color forces is imperative to comprehensively understand the binding mechanism of the ϕ meson to a nucleus [85,175]. The future experiments at J-PARC E16 Collaboration aim to investigate the potential existence of a ϕ-nucleus bound state and quantify the system's binding energy [176]. This may be achieved by generating predominantly slow-moving ϕ mesons, where the most significant nuclear matter influence is anticipated [177]. The varying potentials experienced by kaons and antikaons hold particular significance in the context of neutron-rich heavy-ion beams, especially in experiments such as the Compressed Baryonic Matter (CBM) experiment at the forthcoming FAIR project [16] at GSI, Germany, and in proposed experiments at the Rare Isotope Accelerator (RIA) laboratory in the USA.

Funding The authors sincerely acknowledge the support towards this work from the Ministry of Science and Human Resources (MHRD),

Government of India via Institute fellowship under the National Institute of Technology Jalandhar.

Data Availability Statement My manuscript has no associated data. [Authors' comment: Data sharing not applicable to this article as no datasets were generated or analysed during the current study.]

Code Availability Statement Code/software cannot be made available for reasons disclosed in the code availability statement. [Authors' comment: Code/Software sharing not applicable to this article as no code/software was generated or analysed during the current study.]

Open Access This article is licensed under a Creative Commons Attribution 4.0 International License, which permits use, sharing, adaptation, distribution and reproduction in any medium or format, as long as you give appropriate credit to the original author(s) and the source, provide a link to the Creative Commons licence, and indicate if changes were made. The images or other third party material in this article are included in the article's Creative Commons licence, unless indicated otherwise in a credit line to the material. If material is not included in the article's Creative Commons licence and your intended use is not permitted by statutory regulation or exceeds the permitted use, you will need to obtain permission directly from the copyright holder. To view a copy of this licence, visit http://creativecommons.org/licenses/by/4.0/.
Funded by SCOAP[3].

References

1. P. Haensel, Acta Phys. Polon. B.-Poland **18**, 739 (1987)
2. D.J. Gross, R.D. Pisarski, L.G. Yaffe, Rev. Mod. Phys. **53**, 43 (1981)
3. J.I. Kapusta, K.A. Olive, Nucl. Phys. A **408**, 478 (1983)
4. J. Letessier, J. Rafelski, *Hadrons and Quark-gluon Plasma* (Cambridge University Press, Cambridge, 2002)
5. K.S. Lee, M. Rhoades-Brown, U. Heinz, Phys. Rev. C **37**, 1452 (1988)
6. C. Roberts, Prog. Part. Nucl. Phys. **61**, 50 (2008)
7. I. Pushkina et al., Phys. Lett. B **609**, 265 (2005)
8. B. Holzenkamp, K. Holinde, J. Speth, Nucl. Phys. A **500**, 485 (1989)
9. M. Mannarelli, R. Rapp, Phys. Rev. C **72**, 064905 (2005)
10. R.S. Hayano, T. Hatsuda, Rev. Mod. Phys. **82**, 2949 (2010)
11. R. Kumar et al., Living Rev. Relativ. **27**, 3 (2024)
12. X. Luo, N. Xu, Nucl. Sci. Tech. **28**, 1 (2017)
13. K. Fukushima, J. Phys. G Nucl. Part. Phys. **35**, 104020 (2008)
14. L. Evans, New J. Phys. **9**, 335 (2007)
15. O. Brüning, H. Burkhardt, S. Myers, Prog. Part. Nucl. Phys. **67**, 705 (2012)
16. M. Durante et al., Phys. Scr. **94**, 033001 (2019)
17. V.E. Fortov, B.Y. Sharkov, H. Stöker, Phys. Usp. **55**, 582 (2012)
18. G. Trubnikov et al., Heavy ion collider facility nica at JINR: status and development, in *Exotic Nuclei: EXON-2012-Proceedings of the International Symposium*, p. 315 (2013)
19. R. Pasechnik, M. Šumbera, Universe **3**, 7 (2017)
20. J. Rafelski, Eur. Phys. J. Spec. Top. **229**, 1 (2020)
21. U. Heinz, (2000). arXiv:hep-ph/0009170
22. S.A. Bass et al., Phys. Rev. C **60**, 021902 (1999)
23. R. Fries, B. Müller, C. Nonaka, S. Bass, Phys. Rev. Lett. **90**, 202303 (2003)
24. S. Cao, G.-Y. Qin, S.A. Bass, Phys. Rev. C **92**, 024907 (2015)
25. A.H. Delsemme, *Our Cosmic Origins: From the Big Bang to the Emergence of Life and Intelligence* (Cambridge University Press, Cambridge, 1998)
26. T. Ferris, *The Whole Shebang: A State of the Universe Report* (Simon and Schuster, New York, 1998)
27. Y. Aoki, G. Endrődi, Z. Fodor, S.D. Katz, K.K. Szabó, Nature **443**, 675 (2006)
28. S. Gupta, X. Luo, B. Mohanty, H.G. Ritter, N. Xu, Science **332**, 1525 (2011)
29. C. Bernard et al., Phys. Rev. D **71**, 034504 (2005)
30. S. Gupta, Pramana **63**, 1211 (2004)
31. K. Nagata, Prog. Part. Nucl. Phys. 103991 (2022)
32. G. Gagliardi, W. Unger, Phys. Rev. D **101**, 034509 (2020)
33. R. Iwami et al. (H. QCD Collaboration), Phys. Rev. D **92**, 094507 (2015)
34. P. Huovinen, P. Petreczky, Nucl. Phys. A **837**, 26 (2010)
35. T. Hatsuda, S.H. Lee, Phys. Rev. C **46**, R34 (1992)
36. A. Bochkarev, J. Kapusta, Phys. Rev. D **54**, 4066 (1996)
37. K. Tsushima, K. Saito, J. Haidenbauer, A.W. Thomas, Nucl. Phys. A **630**, 691 (1998)
38. B.-J. Schaefer, J. Wambach, Nucl. Phys. A **757**, 479 (2005)
39. S.R. Wadia, Phys. Rev. D **24**, 970 (1981)
40. T. Waas, N. Kaiser, W. Weise, Phys. Lett. B **379**, 34 (1996)
41. K. Fukushima, Phys. Lett. B **591**, 277 (2004)
42. H. Mao, J. Jin, M. Huang, J. Phys. G Nucl. Part. Phys. **37**, 035001 (2010)
43. B.-J. Schaefer, J.M. Pawlowski, J. Wambach, Phys. Rev. D **76**, 074023 (2007)
44. K. Fukushima, V. Skokov, Prog. Part. Nucl. Phys. **96**, 154 (2017)
45. G. Endrődi, J. High Energy Phys. **2013**, 1 (2013)
46. J. Peterson et al., Phys. Rev. D **108**, 063011 (2023)
47. M. Strickland, V. Dexheimer, D.P. Menezes, Phys. Rev. D **86**, 125032 (2012)
48. A. Bhattacharyya, R. Ray, S. Samanta, S. Sur, Phys. Rev. C **91**, 041901 (2015)
49. N. Magdy, M. Csanád, R.A. Lacey, J. Phys. G Nucl. Part. Phys. **44**, 025101 (2017)
50. J. Braun, B. Klein, B.-J. Schaefer, Phys. Lett. B **713**, 216 (2012)
51. P.H. Cardoso, T. Nunes da Silva, A. Deppman, D.P. Menezes, Eur. Phys. J. A **53**, 1 (2017)
52. J. Rożynek, G. Wilk, J. Phys. G Nucl. Part. Phys. **36**, 125108 (2009)
53. M. Ruggieri, G. Peng, Phys. Rev. D **93**, 094021 (2016)
54. M. Ruggieri, Z.-Y. Lu, G.-X. Peng, Phys. Rev. D **94**, 116003 (2016)
55. R. Nasseripour et al., Phys. Rev. Lett. **99**, 262302 (2007)
56. D.P. Weygand, C. Djalali, R. Nasseripour, M. Wood, Int. J. Mod. Phys. A **22**, 380 (2007)
57. C. Gale, D. Seibert, J. Kapusta, Phys. Rev. D **56**, 508 (1997)
58. F. Karsch, J. Phys. Conf. Ser. **46**, 122 (2006)
59. R. Muto et al., Phys. Rev. Lett. **98**, 042501 (2007)
60. T. Ishikawa et al., Phys. Lett. B **608**, 215 (2005)
61. D. Cabrera, M.V. Vacas, Phys. Rev. C **67**, 045203 (2003)
62. S.S. Adler et al., Phys. Rev. C **72**, 014903 (2005)
63. A. Mishra et al., Phys. Rev. C **69**, 024903 (2004)
64. B. Kämpfer, O. Pavlenko, S. Zschocke, Eur. Phys. J. A-Hadrons Nucl. **17**, 83 (2003)
65. P. Gubler, in *Proceedings of the 14th International Conference on Meson-Nucleon Physics and the Structure of the Nucleon*, p. 020004 (2017)
66. L. Xia, C. Ko, L. Xiong, J. Wu, Nucl. Phys. A **485**, 721 (1988)
67. C.M. Ko, P. Levai, X. Qiu, C. Li, Phys. Rev. C **45**, 1400 (1992)
68. N. Chaudhuri, S. Ghosh, S. Sarkar, P. Roy, Phys. Rev. D **103**, 096021 (2021)
69. R. Mondal, N. Chaudhuri, S. Ghosh, S. Sarkar, P. Roy, Phys. Rev. D **107**, 036017 (2023)

70. N. Sadooghi, F. Taghinavaz, Ann. Phys. **376**, 218 (2017)
71. L. Xiong, Z. Wu, C. Ko, J. Wu, Nucl. Phys. A **512** (1990)
72. W. Chung, C. Ko, G.-Q. Li, Nucl. Phys. A **641**, 357 (1998)
73. M.I. Gorenstein, M. Gaździcki, K.A. Bugaev, Phys. Lett. B **567**, 175 (2003)
74. C. Alt et al., Phys. Rev. C **77**, 024903 (2008)
75. X. Fang, C.M. Ko, G. Brown, V. Koch, Phys. Rev. C **47**, 1678 (1993)
76. A.E. Nelson, D.B. Kaplan, Phys. Lett. B **192**, 193 (1987)
77. A. Mishra, S. Schramm, Phys. Rev. C **74**, 064904 (2006)
78. D. Kaplan, A. Nelson, Phys. Lett. B **175**, 57 (1986)
79. R. Kumar, A. Kumar, SciPost Phys. Proc. **8**, 055 (2022)
80. A. Mishra, A. Kumar, S. Sanyal, V. Dexheimer, S. Schramm, Eur. Phys. J. A **45**, 169 (2010)
81. G.-Q. Li, C. Ko, Nucl. Phys. A **582**, 731 (1995)
82. W.-S. Chung, *Subthreshold Phi Meson Production in Heavy-ion Collisions and Medium Effects in Nuclear Matter* (Texas A&M University, College Station, 1998)
83. J. Cobos-Martínez, K. Tsushima, G. Krein, A.W. Thomas, Phys. Rev. C **96**, 035201 (2017)
84. R. Kumar, A. Kumar, Phys. Rev. C **102**, 045206 (2020)
85. J. Cobos-Martínez, K. Tsushima, G. Krein, A. Thomas, Phys. Lett. B **771**, 113 (2017)
86. G. Vujanovic, J. Ruppert, C. Gale, Phys. Rev. C **80**, 044907 (2009)
87. R. Ferreira et al., Nucl. Phys. A **544**, 497 (1992)
88. M. Mazzoni et al., Nucl. Phys. A **566**, 95 (1994)
89. D. Grasso, H.R. Rubinstein, Phys. Rep. **348**, 163 (2001)
90. J. Braithwaite, H. Spruit, Astron. Astrophys. **450**, 1097 (2006)
91. C.Y. Vallgren et al., Phys. Rev. Spec. Top. Accel. Beams **14**, 071001 (2011)
92. W.-J. Fu, Phys. Rev. D **88**, 014009 (2013)
93. T. Vachaspati, Phys. Lett. B **265**, 258 (1991)
94. L.M. Widrow et al., Space Sci. Rev. **166**, 37 (2012)
95. V. Skokov, A.Y. Illarionov, V. Toneev, Int. J. Mod. Phys. A **24**, 5925 (2009)
96. Y. Zhong, C.-B. Yang, X. Cai, S.-Q. Feng, Chin. Phys. C **39**, 104105 (2015)
97. B. McInnes, Nucl. Phys. B **892**, 49 (2015)
98. M. Ferreira, P. Costa, O. Lourenço, T. Frederico, C. Providência, Phys. Rev. D **89**, 116011 (2014)
99. K. Klimenko, Zeitschrift für Physik C Part. Fields **54**, 323 (1992)
100. S. Klevansky, R.H. Lemmer, Phys. Rev. D **39**, 3478 (1989)
101. G. Bali et al., J. High Energy Phys. **2012**, 1 (2012)
102. K. Fukushima, Views of the chiral magnetic effect, in *Strongly Interacting Matter in Magnetic Fields*, p. 241 (Springer, 2013)
103. R. Ghosh, N. Haque, Phys. Rev. D **105**, 114029 (2022)
104. G.P. Kadam, Mod. Phys. Lett. A **30**, 1550031 (2014)
105. J.P. Carlomagno, D.G. Dumm, S. Noguera, N.N. Scoccola, Phys. Rev. D **106**, 074002 (2022)
106. A.N. Tawfik, A.M. Diab, M. Hussein, Chin. Phys. C **43**, 034103 (2019)
107. R.M. Aguirre, Eur. Phys. J. A **55**, 28 (2019)
108. S. De, P. Parui, A. Mishra, Phys. Rev. C **107**, 065204 (2023)
109. A. Mukherjee, S. Ghosh, M. Mandal, S. Sarkar, P. Roy, Phys. Rev. D **98**, 056024 (2018)
110. J.I. Kapusta, C. Gale, *Finite-Temperature Field Theory: Principles and Applications* (Cambridge University Press, Cambridge, 2007)
111. P. Parui, A. Mishra, Phys. Rev. D **108**, 114025 (2023)
112. R. Kumar, A. Kumar, Chin. Phys. C **43**, 124109 (2019)
113. R. Kumar, A. Kumar, Phys. Rev. C **101**, 015202 (2020)
114. R. Kumar, R. Chhabra, A. Kumar, Eur. Phys. J. A **56**, 1 (2020)
115. D. Zschiesche et al., Nucl. Phys. A **663**, 737 (2000)
116. A. Mishra, A. Kumar Singh, N. Singh Rawat, P. Aman, Eur. Phys. J. A **55**, 1 (2019)
117. P. Papazoglou, S. Schramm, J. Schaffner-Bielich, H. Stoecker, W. Greiner, Phys. Rev. C **57**, 2576 (1998)
118. R. Crewther, Phys. Lett. B **33**, 305 (1970)
119. A. Misra, C. Gale, Eur. Phys. J. C **80**, 620 (2020)
120. D. Zschiesche et al., HNPS Adv. Nucl. Phys. **9**, 170 (1998)
121. A. Faessler et al., Symmetries in intermediate and high energy physics, vol. 163, p. 129 (2000)
122. P. Papazoglou et al., Phys. Rev. C **59**, 411 (1999)
123. D. Zschiesche, Description of Hot, Dense, and Strange Hadronic Matter in a Chiral SU(3) L$\times$ SU(3) R σ-Model, PhD thesis, Thesis (1997)
124. N. Cruz-Camacho et al., (2024). arXiv:2409.06837
125. T. Brauner, Symmetry **2**, 609 (2010)
126. J. Schechter, Phys. Rev. D **21**, 3393 (1980)
127. H. Pagels, Phys. Rev. D **19**, 3080 (1979)
128. G. Hooft, Naturalness, chiral symmetry, and spontaneous chiral symmetry breaking, in *Recent Developments in Gauge Theories*, p. 135 (Springer, 1980)
129. A. Le Yaouanc, L. Oliver, O. Pene, J.-C. Raynal, Phys. Rev. D **29**, 1233 (1984)
130. A. Broderick, M. Prakash, J. Lattimer, Phys. Lett. B **531**, 167 (2002)
131. S. Tiwari, R. Kumar, M. Kumari, A. Kumar, Eur. Phys. J. Plus **139**, 1 (2024)
132. R. Kumar, A. Kumar, Eur. Phys. J. C **79**, 1 (2019)
133. A. Broderick, M. Prakash, J. Lattimer, Astrophys. J. **537**, 351 (2000)
134. A. Mishra, A. Kumar, S. Sanyal, S. Schramm, Eur. Phys. J. A **41**, 205 (2009)
135. G. Mao et al., Phys. Rev. C **59**, 3381 (1999)
136. A. Mishra, E.L. Bratkovskaya, J. Schaffner-Bielich, S. Schramm, H. Stoecker, Phys. Rev. C **70**, 044904 (2004)
137. T. Barnes, E.S. Swanson, Phys. Rev. C **49**, 1166 (1994)
138. G. Brown, C.-H. Lee, M. Rho, V. Thorsson, Nucl. Phys. A **567**, 937 (1994)
139. A. Mishra, S. Schramm, W. Greiner, Phys. Rev. C **78**, 024901 (2008)
140. C.N. Leung, S.-Y. Wang, Ann. Phys. **322**, 701 (2007)
141. E.J. Ferrer, V. de la Incera, I. Portillo, M. Quiroz, Phys. Rev. D **89**, 085034 (2014)
142. S. Fayazbakhsh, N. Sadooghi, Phys. Rev. D **83**, 025026 (2011)
143. F. Bruckmann et al., Phys. Rev. D **96**, 074506 (2017)
144. J.-P. Blaizot, E.S. Fraga, L.F. Palhares, Phys. Lett. B **722**, 167 (2013)
145. D.T. Son, M.A. Stephanov, Phys. Rev. D **66**, 076011 (2002)
146. M. Ishii, H. Kouno, M. Yahiro, Phys. Rev. D **95**, 114022 (2017)
147. B. Sheng, Y. Wang, X. Wang, L. Yu, Phys. Rev. D **103**, 094001 (2021)
148. F. Klingl, N. Kaiser, W. Weise, Zeitschrift für Physik A Hadrons Nucl. **356**, 193 (1986)
149. K.A. Olive et al., Chin. Phys. C **38**, 090001 (2014)
150. G. Krein, A. Thomas, K. Tsushima, Phys. Lett. B **697**, 13 (2011)
151. F. Close, E. Swanson, Phys. Rev. D **72**, 094004 (2005)
152. H. Leutwyler, A.V. Smilga, Nucl. Phys. B **342**, 302 (1990)
153. C. Dominguez, M. Loewe, J. Rojas, Phys. Lett. B **320**, 377 (1994)
154. W. Smith, K.L. Haglin, Phys. Rev. C **57**, 1449 (1998)
155. C. Dominguez, M. Loewe, Y. Zhang, Phys. Rev. D **86**, 034030 (2012)
156. W. Smith, K.L. Haglin, Phys. Rev. C **57**, 1449 (1998)
157. E. Santini, G. Burau, A. Faessler, C. Fuchs, Eur. Phys. J. A **28**, 187 (2006)
158. L. Alvarez-Ruso, V. Koch, Phys. Rev. C **65**, 054901 (2002)
159. V. Koch, Phys. Lett. B **337**, 7 (1994)
160. E. Friedman, A. Gal, C. Batty, Nucl. Phys. A **579**, 518 (1994)
161. L. Tolos et al., Nucl. Phys. A **690**, 547 (2001)
162. M.F. Lutz, C. Korpa, Nucl. Phys. A **700**, 309 (2002)

163. S. Banik, D. Bandyopadhyay, Phys. Rev. C **63**, 035802 (2001)
164. D. Menezes, P.K. Panda, C. Providencia, Phys. Rev. C **72**, 035802 (2005)
165. A. Mishra, S. Misra, Int. J. Mod. Phys. E **30**, 2150014 (2021)
166. T. Cohen, R. Furnstahl, D. Griegel, X. Jin, Prog. Part. Nucl. Phys. **35**, 221 (1995)
167. E. Drukarev, E. Levin, Nucl. Phys. A **511**, 679 (1990)
168. A. Mishra, A. Kumar, P. Parui, S. De, Phys. Rev. C **100**, 015207 (2019)
169. G.-Q. Li, C.M. Ko, Nucl. Phys. A **582**, 731 (1995)
170. A. Polyanskiy et al., Phys. Lett. B **695**, 74 (2011)
171. E.Y. Paryev, J. Phys. G Nucl. Part. Phys. **36**, 015103 (2008)
172. M. Oertel, M. Hempel, T. Klähn, S. Typel, Rev. Mod. Phys. **89**, 015007 (2017)
173. L. Tolos, M. Centelles, A. Ramos, Astrophys. J. **834**, 3 (2016)
174. P.B. Demorest, T. Pennucci, S. Ransom, M. Roberts, J. Hessels, Nature **467**, 1081 (2010)
175. X.-Y. Wang, C. Dong, Q. Wang, Chin. Phys. C **47**, 014106 (2023)
176. K. Aoki et al., Few-Body Syst. **64**, 63 (2023)
177. M. Naruki, Prog. Theor. Exp. Phys. **2012**, 02B013 (2012)